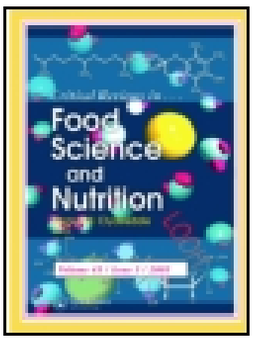

Critical Reviews in Food Science and Nutrition

ISSN: 1040-8398 (Print) 1549-7852 (Online) Journal homepage: http://www.tandfonline.com/loi/bfsn20

Research advances on structural characterization of resistant starch and its structure-physiological function relationship: A review

Zhen Ma & Joyce I. Boye

To cite this article: Zhen Ma & Joyce I. Boye (2017): Research advances on structural characterization of resistant starch and its structure-physiological function relationship: A review, Critical Reviews in Food Science and Nutrition, DOI: 10.1080/10408398.2016.1230537

To link to this article: https://doi.org/10.1080/10408398.2016.1230537

Accepted author version posted online: 19 Sep 2016.
Published online: 02 Jun 2017.

CRITICAL REVIEWS IN FOOD SCIENCE AND NUTRITION
https://doi.org/10.1080/10408398.2016.1230537

Research advances on structural characterization of resistant starch and its structure-physiological function relationship: A review

Zhen Ma[a] and Joyce I. Boye[b]

[a]College of Food Engineering and Nutritional Science, Shaanxi Normal University, Xi'an, Shaanxi, China; [b]Food Research and Development Centre, Agriculture and Agri-Food Canada, St. Hyacinthe, Quebec, Canada

ABSTRACT

Resistant starch (RS) is defined as the fraction of starch that escapes digestion in the small intestine due to either difficult enzyme/starch contact or to the strength of the crystalline regions formed both in native starch and in those retrograded starch. RS occurs naturally in some foods, and some may be generated in others as the results of several processing conditions. Varieties of techniques have been employed to obtain structural characteristics of RS such as their crystallinity, structural order, chain-length distribution and conformation, helicity, and double-helical structures. These structures play an important role in determining the physiological properties of RS such as their prebiotic and hypoglycaemic properties. However, such topic on structural characterization of RS and their structure-physiological function relationship have not been reviewed in previous literatures. Therefore, this review focuses on the past and current achievements of research on structural characterizations of a range of RS prepared from different sources of native starches as a result of a variety of processing conditions. The potential relationships between the structure and the physiological properties of RS, which is of paramount importance for the furtherance understanding and application of RS, are also reviewed in this study.

KEYWORDS

Resistant starch; structural characterization; crystallinity; molecular order; physiological effects; structure-function relationship

Introduction

Resistant starch as promising functional ingredient

Starch, the major component of most plant-originated foodstuff and feedstuffs of numerous industrial raw materials, constitutes an integral part of human staple diets with over 50% of human daily energy intake in agrarian cultures and some 25% of westernized societies (Baghurst et al., 1996). As have been well studied, the digestion of starch occurs partially in the mouth and predominantly in the small intestine where pancreatic α-amylase is released and dextrinase, amyloglucosidase, α-glucosidase, and maltase are embedded in the brush border of the intestinal wall (Sang and Seib, 2006). According to the rate and extent of digestion, starches are classified as rapidly digestible starch (RDS), slowly digestible starch (SDS), and resistant starch (RS). RDS is the starch fraction that causes an increase in blood glucose level immediately after ingestion; SDS is the starch fraction that is digested completely in the small intestine at a lower rate compared with RDS; whereas RS is recognized as the fraction of starch and products of starch degradation that cannot be absorbed by the mammalian digestive enzyme in the small intestine and enters the colon for fermentation (Englyst et al., 1992).

The resistance of starch against the hydrolysis by digestive enzymes in gastrointestinal tract is due to a variety of reasons, as it may be physically inaccessible, retrograded, or chemically modified. Specifically, RS is subdivided into five classes: RS_1 (physically entrapped starch) is a group of inaccessible starch within the whole or partially milled seeds due to lack of cell-wall-degrading enzymes in gastrointestinal tract (Raigond et al., 2015); RS_2 (nongelatinized native starch granule), which is protected from digestion by their compact conformation or structure (as in raw potato, green banana, and native high-amylose maize starch (HAMS)), consist of amylopectin crystals of uncooked native starch granules and is usually in B- or C-type crystalline polymorph (Englyst and Cummings, 1987); RS_3 (retrograded starch) can be produced by gelatinization (i.e., a process of disruption of the granule structure by heating with an excess of water) and retrogradation (i.e., a process of slow recrystallization of starch molecules upon cooling or dehydration) during food processing (Englyst et al., 1992); RS_4 (chemically modified starch) can be prepared by etherification, esterification, and cross-linking, which cannot be broken down by digestive enzymes (Lunn and Buttriss, 2007); RS_5 (amylose-lipid complex) can be formed assuming that the aliphatic part of lipid is included inside the amylose helix in the case of amylose-lipid complexes, which requires higher temperatures for gelatinization, while the polar group of lipid lies outside, which is too large to be included (Morrison et al., 1993). The amylose molecules, particularly with the presence of lipids, can also entangle with amylopectin to maintain the integrity of starch granule during heating and shearing (Jane, 2006). Among these

CONTACT Zhen Ma zhen.ma@mail.mcgill.ca College of Food Engineering and Nutritional Science, Shaanxi Normal University, Xi'an, Shaanxi, 710062, China.
Color versions of one or more of the figures in the article can be found online at www.tandfonline.com/bfsn.

RS categories, RS_1 level can be reduced by treatments that destroy the physical barriers in foods (e.g., grinding and protease hydrolysis), whereas being heat stable, RS_1 does not break down during normal cooking. RS_2 content can be reduced after applying thermal treatments, although some RS_2, in case of HAMS, has been reported to be stable and can maintain its enzymatic resistance under commonly used food processing conditions (Thompson, 2000; Wang et al., 2001). RS_3 seems to be of particular interest due to its preserved nutritional functionality and thermal stability during cooking (especially retrograded amylose crystals), which thus allows RS to endure heat treatment during cooking and enables its wide applications as food ingredient.

A number of advantages of using RS as commercial ingredients in the applications of a variety of foods are presented in the following aspects: (i) the fact of being derived from natural botanical sources, (ii) and the performance of excellent functional properties including low-water-holding capacity, white color, bland flavor, and small particle size (i.e., low interference in texture), both make RS a high-promising potential ingredient to be incorporated into a number of food products with better acceptability and greater palatability than those prepared with traditional fibers. According to previous studies (Sharma et al., 2008), an improved crispness, expansion, mouth feel, color, and flavor are observed for food products prepared with RS including baked products, pasta/noodles, breads, snacks, and beverages. Additionally, good extrusion and film-forming qualities are also reported for RS supplemented foods which are superior to traditional fiber-enriched products (Nugent, 2005).

RS cannot be readily digested as the ordinary starch, which leads to its great biological importance. RS can affect body weight and energy balance (Lösel and Claus, 2005) and increase lipid excretion to reduce calorie intake and decrease serum lipid levels. Since RS has zero calories, and, when used as a low-calorie food additive, can control weight effectively and thus are beneficial for people with obesity. The ingestion of RS can decrease insulin secretion and control postprandial blood glucose to prevent diabetes (Weickert et al., 2005). The Food and Agriculture Organization has listed RS as a dietary fiber that can be used for the prevention of type-II diabetes mellitus in 1990 (DeVries, 2004). The prebiotic properties of RS have also drawn researcher's attention recently. Several studies found that RS stimulates the growth of beneficial bacteria in the gut (e.g., *bifidobacteria*) and modulate gut immune function and microbiota activity by decreasing the concentration of secondary bile acids, ammonia and phenol content, due to an increase in short-chain fatty acids (SCFAs) levels (especially butyric acid) produced by the fermentation of RS by the gut microflora in the colon (Fuentes-Zaragoza et al., 2011). RS can also lower the intestinal pH and promote the absorption of zinc, calcium, and magnesium ions (Yonekura and Suzuki, 2005).

Mechanism of resistant starch formation during processing

The enzymatic resistant nature of starch is determined by multiple factors including size of granules, shape of granule surface, size of pores in the starch granule, amylose/amylopectin ratio, the chain length of amylose, linearization of amylopectin, and starch crystallinity (Leszczyñski, 2004; Sajilata et al., 2006). In addition, the RS content is not permanently stable which varies during postharvest (Wang et al., 2014) and kernel development (Jiang et al., 2010c). The applications of processing and storage conditions of the processed foods also have a significant impact (García-Rosas et al., 2009). Generally, RS can be formed by decreasing the enzyme susceptibility of starches during processing under different temperatures with varied treatment time, which have been thoroughly studied by previous researchers for starches from different botanical origins and with varying amylose/amylopectin ratios. For instance, the production of RS can be generally achieved by both thermal and enzymatic methods as well as with a combination of both, which involves the starch gelatinization and retrogradation. Autoclaving, extrusion, baking, and microwave irradiation are common thermal-processing methods applied for starch gelatinization. Followed by which, processing conditions that enhance starch retrogradation such as cooling, or several cooking and cooling cycles, freeze/thaw cycles are used to obtain higher levels of RS. In addition, debranching of amylopectin or molecular-weight-reduction techniques by the action of enzymes (including pullulanase or isoamylase) or partial acid hydrolysis have also been attempted in previous studies. By doing so, a larger number of linear chains could be obtained to provide an increased chance for facilitating paring, molecule alignment or aggregation, which will, thus lead to an easier opportunity for crystallinzation and enhance the yield of retrograded starch and RS production (Polesi and Sarmento, 2011). The chemical modifications such as phosphorylation and hydroxypropylation, acetylation, and oxidation as well as citric acid modification can also be used to produce type4 RS (Chiu et al., 1994; Charalampopoulos et al., 2002; Hasjim and Jane, 2009; Ashwar et al., 2015). Depending on the severity of processing conditions, the starch digestibility is either increased, due to complete gelatinization of starch, or decreased, due to following retrogradation upon cooling. The extent of starch gelatinization and retrogradation occurring during process determines the formation of undigested starch, and its subsequent metabolic responses (Mangala et al., 1999b). The degree of debranching also has a great impact on RS formation. For instance, linear fragments with degree of polymerization (DP) of 100–300 glucose units are preferably produced after starch debranching. The RS yield tends to be low when DP is less than 100 glucose units since the polymers are not long enough to form enzyme-resistant crystallites. On the other hand, linear chains polymers with DP higher than 300 also cannot effectively align to form enzyme-resistant crystallites when insufficient hydrolysis of starch occurs (Eerlingen et al., 1993b; Onyango et al., 2006).

Following by various processing treatments, the RS can then be obtained by isolation via both *in vitro* and *in vivo* methods, the *in vitro* quantification of RS refers to the analysis of RS content outside a living organism (enzyme RS, ERS) as the part after digestion of processed food products, whereas *in vivo* methodology involves obtaining undigested starch fraction from ileostomy subjects or the intubation procedure (physiological RS, PRS) (Faraj et al., 2004). Up till now, the majority of RS studies involve the obtaining of RS fraction from *in vitro*

digestion methods. According to Mangala et al. (1999a), PRS and ERS have almost comparable M_w values based upon gel permission chromatograph observation. However, according to the studies conducted by Faisant et al. (1993), the PRS appeared to consist of three fractions: a first population of high-molecular-weight α-glucans attributed to amorphous potentially digestible material, a second made of B-type-retrograded amylose crystallites, and a third containing oligosaccharides. Whereas the *in vitro* RS fractions showed no high-molecular-weight molecules due to more extensive hydrolysis in the *in vitro* procedure. The conformational changes could happen during the digestion process (Lopez-Rubio et al., 2008b), where amylose chains are rearranged into enzyme-resistant structures of higher crystallinity and increased molecular order. Therefore, the factors including kinetics of enzyme hydrolysis and kinetics of amylose retrogradation should be both considered, which leads to the resistance to enzyme digestion of a specific processed starch.

Enzymatic resistance mechanism of resistant starch

Although essentially, RS is still a homopolysaccharide consisting of a number of monosaccharide units linked together with α-Glc(1→4) and α-Glc(1→6) linkages. The proposed mechanisms for the resistance of RS to amylolysis are the formation of their conformational characteristics consisting any one of a number of possible states including crystalline amylose, crystalline amylopectin, and noncrystalline (yet associated) amylose or amylose-lipid complex as well as, in some cases, the highly branched clusters of branch points. The crystalline regions generally are made up of double helices which lower the vulnerability of starch by decreasing the effective surface and thus hinder the diffusion and adsorption of enzymes onto the starch substrate. The noncrystalline structure, on the other hand, is often presented when the entrapment of amorphous region is within imperfect crystals and the acquisition of noncrystalline double-helical order due to hindrance to enzymatic attack that is brought about by these structures (Cairns et al., 1995; Gidley et al., 1995). Several studies imply that the low crystallinity does not always necessarily link with the easily digestible fraction. The RS fraction could contain both the crystalline and amorphous regions, i.e., simple helix can be organized in either the crystalline phase or dispersed in an amorphous phase. Lamellla model and micelle model have been proposed previously to describe the schematic presentation of enzymatic resistant structure of the retrograded starch (i.e., RS_3) as shown in Figures 1a and b, respectively (Sajilata et al., 2006). The blocklet model (Figure 1c), as proposed by describing the large "blocklets" formed by double helices, is responsible for the enzymatic resistance of raw potato starch (Gallant et al., 1997). In some cases, the enzyme-resistant fractions could consist of combined (very) short nonordered branches and longer stretches of

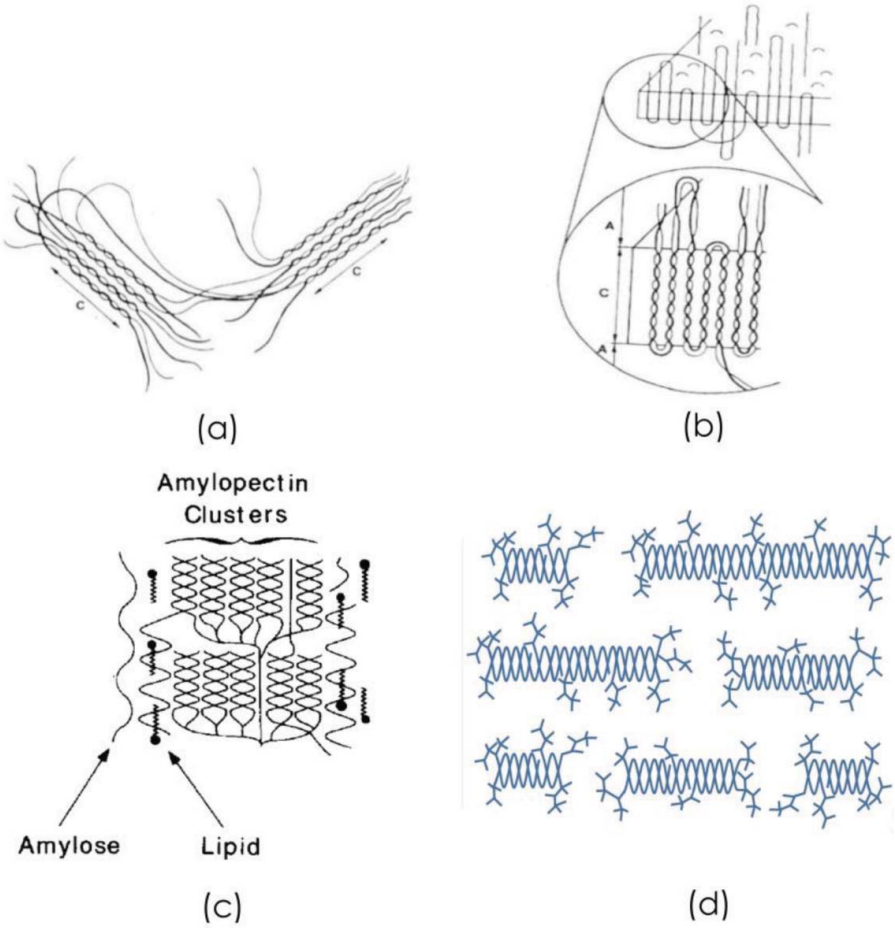

Figure 1. (a) The micelle model of RS_3, where C represents for crystalline region (Sajilata et al., 2006); (b) lamella model of RS_3 (Sajilata et al., 2006); (c) blocklet model of RS_2 (Gallant et al., 1997); (d) fringed micelle structure of RS (Shrestha et al., 2015).

glucan chains that can form double helices (in some cases single helices). Shrestha et al. (2015) has proposed a fringed micelle model for RS from processed HAMSs (Figure 1d), which is based on lateral aggregation and enzyme susceptibility, both limited by attached clusters and branched points based on the structure of residual material after long-time digestion. The residual clusters of branch points coat the surface of (mostly) double helices, which thus limiting lateral aggregation.

Measurement of the structure of resistant starch

A variety of techniques including X-ray diffraction (XRD)analysis, small-angel X-ray scattering (SAXS), solid-state ^{13}C-nuclear magnetic resonance (^{13}C-NMR), Fourier transform infrared spectroscopy (FT-IR), gas chromatography-mass spectrometry (GC-MS), high-performance size exclusion chromatograph (HPSEC), gel permeation chromatograph (GPC), high-performance anion-exchange chromatograph (HPAEC), fluorophore-assisted carbohydrate electrophoresis (FACE), differential scanning calorimetry (DSC), and scanning electron microscopy (SEM) have been attempted to explain the structural characteristics of RS. Some selected structural characterization techniques in relation to the hierarchical structure of starch are presented in Figure 2. For instance, XRD can be applied to investigate different patterns of crystalline structure and crystallinity of RS obtained from various botanical source and/or formed under different conditions and gives information on long-range molecular order information; FT-IR, on the other hand, is sensitive to short-range molecular order (i.e., changes in amorphous and crystallinity region) and the changes in chain conformation, helicity, double-helical structure, and changes in combinations of hydrogen bonds generated during the formation of RS; SAXS can be used to determine structural features of RS with crystallinity and double helix regions at the 4–5 nm length scale; solid-state ^{13}C-NMR can provide useful information by giving characteristic spectra for ordered helices and nonordered chains, which can be used to estimate the double helix content into solid starch samples, the spectra are interpreted in terms of a combination of amorphous and helical conformations based on ^{13}CNMR observation, irrespective of whether helicals are present within the crystallites or not, which are comparable and complement to those results obtained from XRD (Goodfellow and Wilson, 1990); HPSEC, GPC, HPAEC, and FACE can be used to measure the molecular-weight distribution and chain-length distribution of RS; the glycosidic linkage pattern of RS can be determined by permethylation followed by GC/MS analysis; the information regarding order-disorder transition processes of RS can be provided by DSC; SEM are generally used to provide topographic features of RS. These techniques, overall, when combined, could provide comprehensive analysis of structural characteristics of RS as well as changes occur during the formation of RS when compared with the structure of their native starches.

Recent reviews on resistant starch

Reviews on the topic of RS have appeared in the past. Earlier researchers Shukla (1996) and Niba (2002) have reviewed the general aspects of RS as a potential functional food ingredient. In a review dating back more than a decade, Haralampu (2000) examined the physical properties and biological impacts of RS_3, the sources of RS are reviewed, with a focus on the principles behind the production of food ingredient highly concentrated in retrograded amylose. Morell et al. (2004) reviewed the strategies to manipulate crop genetics in order to generate additional sources of RS. RSs have also been reviewed by Sharma et al. (2008) on the aspects of both their potential health benefits as well as functional properties to produce high-quality foods. Perera et al. (2010) published a comprehensive review on analytical protocols for determining RS which covered a variety of methodologies for analyzing RS as well as the recent publications describing the influence of starch composition and processing method on variations in RS contents of pulses and cereal

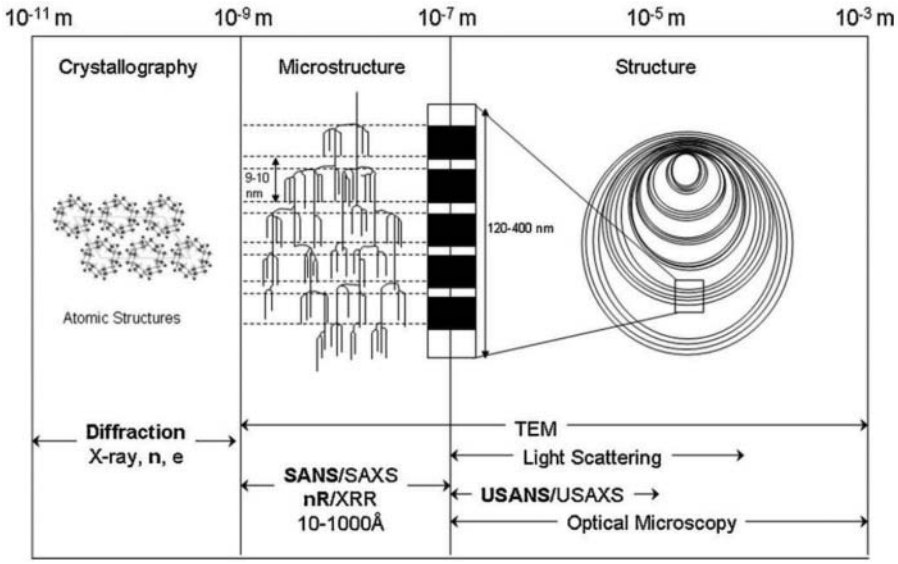

Figure 2. Different techniques in relation to the hierarchical structure of starch; n = neutron; = electron; nR/XRR = neutron and X-ray reflectometry, TEM = transmission electron microscopy; USANS/USAXS = ultra-SANS/SAXS. Reproduced with permission from Lopez-Rubio and Gilbert (2010).

starches. A review by Fuentes-Zaragoza et al. (2011) examined the physiological and functional properties of RS as prebiotics. More recently, Raigond et al. (2015) have reviewed the recent published papers on classification, properties, applications, and health benefits of RS. However, these reviews papers available in the literatures are generally focused on the influence of processing and starch composition on the variation of RS levels in different food sources, the analytical methodologies developed to determine RS content, the potential application of RS in numerous food products as well as the physiological effects of RS. There is a lack of information on reviewing the structural characterization of RS derived from different origins and/or prepared by different processing methods as well as their structure-physiological function relationship. The functionality, nutritional value, and especially the physiological implications of RS from different food origins and/or after applying different processing conditions are all dependent on their structural and conformational characteristics. The variations in physiological effects including the prebiotic properties, the turnover of bile acids, as well as the ability of improving mineral absorption were found to be correlated with the differences in structural conformation and integrity of RS, which underlies the motivation and contexturalizes the objective of this review. Therefore, in this article, both past achievements and current status of research into the in-depth structural characterization of a range of RS prepared from native starches from different sources by the meaning of several techniques including XRD, SAXS, ^{13}C-NMR, GC-MS, FT-IR, HPSEC, HPSEC, GPC, HPAEC, FACE, SEM, transmission electron microscopic (TEM), and DSC are comprehensively reviewed. The paramount importance of learning the structure-physiological functionality relationship of RS for the furtherance understanding and application of RS are also reviewed in this study.

Research advances on structural characterization of resistant starch

Measurement of crystallinity and structural order of RS by X-ray diffraction

The XRD is one of widely used techniques to determine the crystallinity and crystalline-phase composition of RS. The XRD technique generally detects the regularly repeating ordering of helices, thereby reflecting the three-dimensional order of starch crystallinity. This technique, however, is less sensitive to irregularly packed structures, small chain aggregates, or isolated single helices (Gidley and Bociek, 1985). These parts, nevertheless, also represent for an important fraction of enzymatic RS. Therefore, XRD should be applied in a combination of other techniques, such as ^{13}CNMR and SAXS, to provide a comprehensive view of structural characteristics of RS. The XRD and wide-angle X-ray scattering are often regarded as identical techniques in the literature, however is not strictly so. The experimentally obtained XRD patterns are decomposed into a series of discrete diffraction peaks and several broad peaks. The discrete peak often represents for starch with an extended crystal line and complete crystal surface, the sharper the reflection of the peak, the higher the crystallinity of the sample, though the less sharpness of peaks could also be due to poor water-of-hydration values (Mangala et al., 1999b). On the other hand, a wide diffraction peak is characteristic of an amorphous structure when starch contains a small crystal line and incomplete crystals (Zhang et al., 2014). The starch granules generally exhibit four classes of crystalline structures depending on the packing pattern of double helices of the glucan chains in starch granules, referred to as the A, B, C, and V types, and vary in their crystallinity from 15 to 45% depending on plant species (Zobel, 1988). The samples are normally scanned in angular range of 2–40° (2θ) using Cu K_α radiation, the polymorph type is obtained by analyzing the evolution patterns with the appearance of peaks/reflections at 2θ on the X-ray diffractograms as summarized in Table 1. The proportion of each type's (A, B, C, and V) crystallinity can thus be determined by measuring the area under their characteristic peak 2θ divided by the total minus the baseline area. According to previous studies, the degree of crystallinity is determined based on internal or external comparison. The external comparison technique is more useful to determine the relative crystallinities, where the experimental curves are compared with 100% crystallinity and completely amorphous diagrams. On the other hand, during the internal comparison, the areas corresponding to the respective contributions of amorphous and crystalline scattering are evaluated by estimating the baseline by collecting a diffraction pattern from an empty sample holder, which corresponds to the scattering from the instrument and air. The internal comparison thus allows us to determine the absolute crystallinity. However, the values obtained by using internal technique have such discrepancies according to the published values. Therefore, the external comparisons, namely the measurement of relative crystallinities, are often used currently by researchers (Buléon et al., 1998; García-Rosas et al., 2009; Mutungi et al., 2011). The differences in the intensities of reflections, the appearance and disappearance of certain peaks at 2θ on X-ray diffractogram thus can be used to indicate the significant qualitative and quantitative differences in crystallinities.

The aforementioned methods of defining the degree of crystallinity are generally based on the "two-phase concept." This concept estimates the degree of crystallinity by decomposing the diffraction pattern into sharp (crystalline) and diffuse (amorphous) components (Morrison et al., 1993), assuming that relatively perfect crystalline domains (crystallites) are interspersed with amorphous regions, without considering the polymeric structures that encompasses intermediate crystalline objects, chain folding, lamellar crystalline growths, lattice dislocations, and other phenomena, which are basically most updated understanding of crystalline structure of RS (Samuels, 1970; Lopez-Rubio et al., 2008a). Therefore, a "crystal-defect concept" opposed to "two-phase concept" has been proposed by Alexander (1969), which considers the scenario that a portion of the X-ray scattering from the crystalline domains is diffuse and contributes to the so-called amorphous background. The proper decomposition of crystalline and amorphous intensity profile, which is essential for any methods employed for crystallinity calculation, is normally achieved by a curve-fitting technique, in which the crystalline and amorphous components are assumed to be a Gaussian, Lorentzian, Voigt (combination of Lorentzian and Gaussian line shapes) or other related functions (Cao et al., 1999). A peak-fitting technique with crystal-

Table 1. Typical peaks of 2θ obtained from X-ray diffractogram and their corresponding types/characteristics of polymorph.

Types of polymorph	Typical peaks of 2θ obtained from X-ray diffractogram[a] (deg)	Auxiliary peak of 2θ obtained from X-ray diffractogram[a] (deg)	Chain characteristics[b]	Branch-chain characteristics[c]
Type A	15.11 17.14 18.14 26.27	9.98 11.19 22.93 23.68 30.30 33.08	Contains amylopectin with chain lengths of 23–29 glucose units. The type A has the formation of outer double-helical structure which is resulted from the hydrogen bonding between the hydroxyl groups of chains of amylopectin molecules. In between these micelles, linear chains of amylose moieties are packed by forming hydrogen bonds with outer linear chains of amylopectin	Consists of amylopectin molecules with larger proportion of shorter average branch chain lengths (DP of 6–12) but a smaller proportion of longer branch chain (DP>12) than that of the B-type polymorph; the branching linkage of amylopectin in the A-type polymorph starch are located in both the amorphous and crystalline regions
Type B	5.51 14.60 16.85	10.01 11.02 13.85 22.30 23.71 26.16 30.61 33.84	Made up of amylopectin with chain lengths of 30–44 glucose molecules with water interspread	Consists of amylopectin molecules with long average branch-chain lengths; the branch linages of amylopectin in the B-type polymorph starch are mostly located in the amorphous region
Type C (combined type A and type B)			Consists of amylopectin with chain length of 26–29 glucose molecules, a combination of type A and type B	Has an average branch-chain length in between that of A- and B-type starches
Type V	19.80	7.40 12.90		

[a]Godet et al. (1995); Lopez-Rubio et al. (2008a); [b]Sajilata et al. (2006); [c]Jane (2004, 2007).

defect concept approach to calculate the crystallinity in granule starch was proposed by Lopez-Rubio et al. (2008a), very similar results are obtained by applying this technique, when comparing the crystallinity values obtained by XRD with the amount of double helices as measured by ^{13}C-NMR.

The A-type polymorph, which corresponds to the A-type XRD pattern, has a monoclinic unit cell and a nearly close-packed arrangement which consist of left-handed parallel stranded double helices (Figure 3a). The B-type polymorph, corresponding to the B-type XRD pattern, has a hexagonal unit cell consisting left-handed parallel stranded double helices and adopts a more open structure and contains more water in its structure (Figure 3b). Some starches such as pea and green banana starches exhibit a C-type XRD pattern, which is a combination of the A- and B-type polymorphs. The V-type polymorph, which is different from the double-helical nature of A- and B-type crystal structures, has been described to result from single amylose helices with some fractions complexed with endogenous granular lipids (Morrison et al., 1993). Typical XRD diagrams of different polymorphs are presented in Figure 4 and their corresponding chain and branch chain characteristics are summarized in Table 1. The more porous structure of the

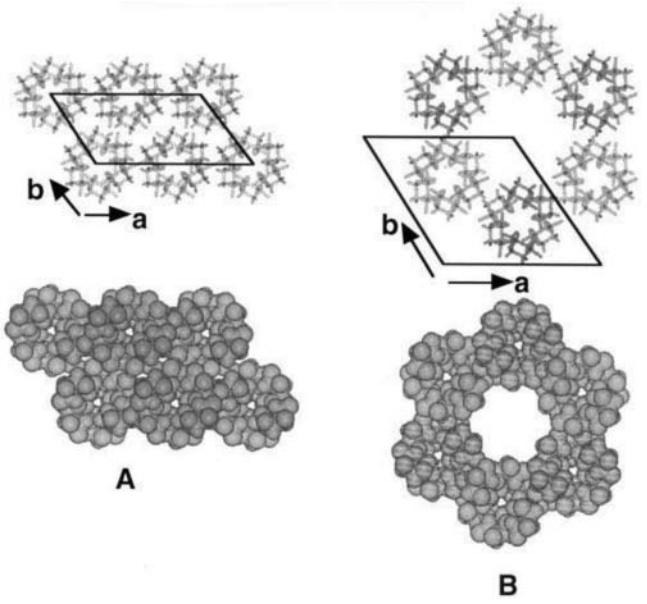

Figure 3. Crystalline packing of double helices in (a) A-type amylose and (b) B-type amylose. Projection of the structure onto the (a, b) plane. Reprinted with permission from Buléon et al. (1998).

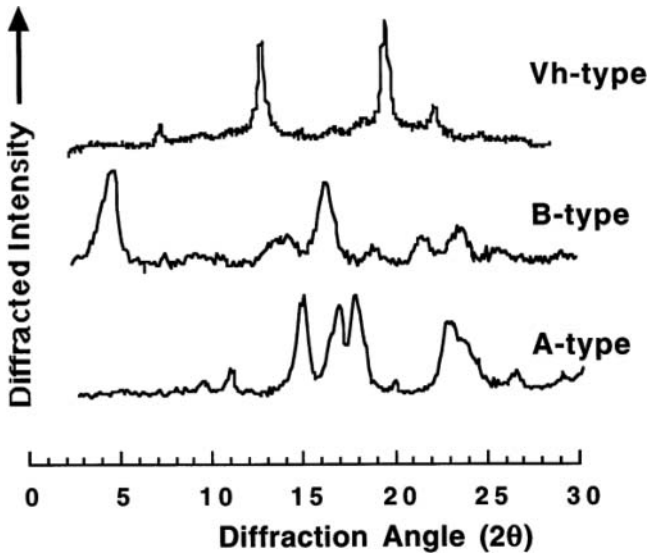

Figure 4. X-ray diffraction diagrams of A, B, and V_h types (V_h: hydrated). Reproduced with permission from Buléon et al. (1998).

A-type polymorph of starch granules than the B types can be explained by differences in their amylopectin structure (Jane, 2006). Studies showed that the starch granules with B or C pattern are generally more resistant to amylolytic digestion than those with A pattern. This difference could be attributed to chain lengths of the branch-chain double helices and the packing of double helices in starch granules (Jiang et al., 2010c) as described in Table 1. As in B-type starch, enzymatic damage is only on the surface of granules, whereas the enzymatic hydrolysis undergoes deeper with A-type crystallinity (Paramahans and Tharanathan, 1982). The RS formation under various processing treatments is often accompanied by alternation of the nature of sample's X-ray polymorph pattern. For example, the process of obtaining RS following by the combined hydrolysis by acid or enzyme and heat treatments changed the crystallinity pattern from C to B according to studies reported by Polesi and Sarmento (2011). Similar changes have also been observed by Yin et al. (2007) and Polesi and Sarmento (2011) in RS prepared by pullulanase debranching, autoclaving, and retrogradation.

The crystallinity plays an important role in starch granule architecture and physicochemical characteristics, such as the susceptibility to enzymes and the indissolubility in cold water. The crystalline polymorphs are greatly dependent on the branch chain length of amylopectin, whereas the crystallinity of starch granule is greatly dependent on the amylopectin component. Especially the short chain fraction of amylopectin has been found to play an important role in starch crystallinity (Cheetham and Tao, 1998). The chain length involved in the crystalline phase and the branching pattern in the amylopectin molecules influence the degree of crystallinity and the crystalline type. The nature of starch crystalline depends on both genetic control and climatic conditions during the plant growth. The variations in degree of crystallinity can be attributed to crystal size, amount of crystallinity, orientation of double helices, and extent of interaction between double helices of RS (Song and Jane, 2000). Hydration of starch also induces an increase in degree of granule crystallinity, without changing the crystal type (Hizukuri et al., 1997; Buléon et al., 1998). According to Xie et al. (2006), the diffraction peaks of characteristic 2θ values generally showed a decreasing tendency in chemically manufactured RS_4 compared with their native starch samples. As in the studies of Sievert et al. (1991), the patterns of RS obtained from incubation with pancreatic α-amylase exhibited a somewhat sharper reflection at 0.537 nm when compared with the X-ray pattern of RS from termamyl-amyloglucosidase incubation, suggesting slightly higher crystallinity.

Different crystal structures can be resulted depending on processing conditions during which RS is formed. The formation of A-type polymorph is favored when at higher temperatures, higher concentrations, with the presence of water-soluble alcohols and organic acids, and the presence of salts of high lyotropic number. The presence of shorter average chain length of the amylose also often leads to the formation of A-type crystal (Gidley, 1987). It was found that an A-type polymorph can be obtained from debranched glycogen (with average chain length of 11.2) crystallized from hot aqueous solution of 50% at 30°C. Whereas lower concentrations or lower temperatures yielded a B- or C-type polymorph. Different recrystallization condition also has an impact on the polymorph type of RS. B-type structure can be formed when the retrogradation of starch gels occurs at room or lower temperature, whereas starch gels that are retrograded above 70°C leads to the formation of crystals that have an A-type pattern, regardless of the original crystalline patterns of the native starch from which it was prepared (Eerlingen et al., 1993a). According to Shamai et al. (2004), the polymorph B with crystallinity much lower than that of the granular form was formed when retrograde at low temperatures, where the lamellas are arranged in long periodicity. Contrary, retrogradation at high temperature leads to formation of polymorphs A and V with no defined periodicity, and the degree of crystallinity is very low. During RS_3 preparation by debranching followed by different methods of recrystallinization (Mutungi et al., 2011), it was found that the temperature cycling and heat-moisture treatments favored A-type crystalline pacing, whereas a higher amount of B-type packing was evident in the annealing samples due to milder recrystallization conditions. Similarly, the V-type crystalline material was found to be significantly higher in the temperature-cycling and heat-moisture-treated samples, which suggested that the higher temperature conditions enabled stabilization of significantly higher amount of single helical chains into entities capable of diffracting X-rays. However, the exact solid concentration and crystallization temperature required to produce A- or B-type polymorph varied depending on specific material. The crystalline types of RS obtained from various sources and prepared by different processing methods are summarized in Table 2.

The general trends observed for XRD results by different researchers suggested that the RS prepared by molecular mass reduction (enzyme or acid) and hydrothermal treatments of native starch involves the cocrystallization of chains of recrystallized amylose and fragments of linear amylopectin (debranching) during heating and cooling, consequently leading to a more intense and orderly crystalline structure (Polesi and Sarmento, 2011). However, the crystallinity is not necessarily proportional to the levels of RS from various origins. And the degree of crystallinity is not always linked to resistance to amylolytic enzymes (Mutungi et al., 2011; Raigond et al., 2015). Based on previous studies, the levels of crystallinity measured in both the ERS obtained *in vitro* and PRS that are obtained *in vivo* fractions have been quite low. The following two hypotheses are generally accepted theories that can justify the enzymatic resistance of the noncrystalline fraction: one is the attributed by the amorphous regions within the imperfect crystals, the other being the resistance of double-helical structures that are not necessarily being part of crystallites. The low X-ray crystallinity is not necessarily related to poorly ordered starch molecules, but may be the result of small-size crystallites in the granules, or originate from a combination of molecular and mesoscopic factors, including both recrystallization and an increase in very short branches (Shrestha et al., 2015).

Measurement of structural order of RS by small-angel X-ray scattering

During the measurement of SAXS, the X-ray photon is elastically scattered by a starch sample and resulting distribution of scattered radiation which can then be analyzed to provide information about the size, shape, and orientation of

Table 2. The crystallinity and molecular weight of RS from various native starch and those prepared by various treatments.

Sources for resistant starch	Processing methods or preparation of RS samples	X-ray polymorphic form	Molecular weight (M_w) or DP_n	References
Legume				
Bengal gram and red gram *dhals*	Pressure cooking followed by refrigeration cooling (four cycles) isolated, and purified by $HClO_4$ solubilization followed by GPC on precalibrated sepharose	C and V types	31.1 and 50.1 KDa	(Mahadevamma et al., 2003)
Red kidney beans (*Phaseolus vulgaris* L.)	(i) enzymatic hydrolysis (pullulanase)	B-type	NA	(Reddy et al., 2013)
	(ii) gelatinized and hydrolyzed by enzyme (autoclaved at 121°C for 30 min, cooled to 4°C for 24 h	(i) relative crystallinity: 41.22% (ii) relative crystallinity: 45.88%		
Lotus seed	(i) Unpurified lotus seed RS (NP-LRS3)	B type	102 KDa (NP-LRS3)	(Zhang et al., 2014)
	(ii) Enzyme-purified lotus seed RS after drying (GP-LRS3) (iii) enzyme-purified lotus seed RS (ZP-LRS3)	crystallinity 79.60% (NP-LRS3) crystallinity 81.65% (GP-LRS3) crystallinity 83.95% (ZP-LRS3)	14 KDa (GP-LRS3) 25 KDa (ZP-LRS3)	
Indica rice	Dual modification-treated starch (the starch was cohydrolyzed with two enzymes (alpha-amylase and pullulanse), then cooled at 4°C overnight	A mixture of B and V types (crystallinity 51.0%)	NA	(Zhou et al., 2014)
Waxy rice	Waxy rice starch slurry was cooked at 95°C for 30 min, then debranched by pullulanase for 12 h	B and V types (the relative crystallinity: 44.1–47.5%)	NA	(Shi and Gao, 2011)
Cassava starch	The gelatinized starch was debranched using pullulanase and then recrystallised by (i) annealing, (ii) temperature-cycling or (iii) heat-moisture treatment, the recrystallized products were subject to in vitro digestion using porcine pancreatic α-amylase and amyloglucosidase	A, B, and V types (for RS rich powder and RS) (i) crystallinities: 40.9% (annealed RS rich powder) crystallinities: 47.9% (annealed RS) (ii) crystallinities: 50.7% (temperature-cycled RS-rich powder) crystallinities: 54.4% (temperature-cycled RS) (iii) crystallinities: 50.7% (heat-moisture-treated RS-rich powder) crystallinities: 58.2% (58.2 RS)	NA	(Mutungi et al., 2011)
Potato starch	Potato starch amylose samples were dissolved in DMSO and phosphate buffer, the solutions were heated at 100°C for 10 min and cooled at 4°C overnight, RS then was isolated by enzymatic-gravimetric method with the using of termamyl[a] enzyme	B pattern	DP of 19–26	(Eerlingen et al., 1993b)
Rice (*Oryza sativa*, Intan variety)	RS was prepared from five-cycle-autoclaved rice flour, isolated with termamyl, protease and amyloglucosidase, and purified by $HClO_4$ and SE-HPLC	B and V types	M_w of 1200 KDa	(Mangala and Tharanathan, 1999)
Maize tortillas	RS was prepared from tortillas starch (stored under refrigerated conditions for 5 and 10 days) by removing digestible starch with heat stable α-amylase, protease, and amyloglucosidase	B type (crystallinity for RS in tortillas stored for 5 and 10 days were of 7.5 and 12.5%, respectively)	NA	(García-Rosas et al., 2009)
Ragi starch (Finger millet, *Eleusine coracana*)	From five-cycle-autoclaved finger millet flour, RS was isolated by sequential enzymatic digestion and purification by GPC and HPSEC	B and V types	M_w of 1400 KDa	(Mangala et al., 1999a)
Native and amylomaize starch	RS was prepared by repeated cycles of autoclaving and cooling and was isolated with termamyl and amyloglucosidase	B pattern	NA	(Sievert et al., 1991)
Rice (*Oryza sativa*, Intan variety)	RS was prepared from five-cycle-autoclaved rice, isolated by hydrolysis with termamyl, protease, and amyloglucosidase, and purified by HPSEC	B and V types	1.2×10^6 Da	(Mangala and Tharanathan, 1999)
Maize amylose-extender (ae) mutant starch	Enzymatic hydrolysis of native ae-line starches at 95–100°C	B-type Crystallinities: 21.9–24.1% (GEMS-0067 ae-lines); Crystallinities: 15.0–16.0% (existing ae-lines)		(Jiang et al., 2010a)
Chickpea starch	RS was prepared by molecular mass reduction with puululanase enzyme or acid and hydrothermal treatments of autoclaving (121°C/30 min), stored under refrigeration (4°C/24 h), and lyophilized	B type Crystallinity: 29.14–45.56% (chickpea RS prepared by subjecting to different treatments)		(Polesi and Sarmento, 2011)

[a]Termamyl, a thermostable α-amylase from *Bacillus licheniformis*; DP represents for degree of polymerization; HPSEC stands for high-performance size exclusion chromatograph.

components in the sample. The SAXS technique is useful for structural determination at low resolution for systems that do not necessarily have long-range crystalline order. The assessment of crystallinity as determined by SAXS is fundamentally different with XRD, as XRD determines dimensions generally associated with interhelix order whereas SAXS typically measures order along the chains (Blazek and Gilbert, 2011). A law of reciprocity giving an inverse relationship between the size or dimension of the scattering object and associated scattering angel (via Bragg's law to yield a real-space dimension, $d = 2\pi/q$) is used to characterize the scattering (Chanvrier et al., 2007; Blazek and Gilbert, 2011). The semicrystalline structures are normally formed by a lamellar structure of alternating crystalline and amorphous regions with regular repeat distance of 9–10 nm^{-1} (with corresponded q of 0.6–0.7 $Å^{-1}$) as detected by SAXS (Cameron and Donald, 1992). The SAXS measures the scattered intensity versus the magnitude of the scattering vector, q, ranging from 0.02 to 0.3 $Å^{-1}$, which is defined by the following equation (Eq. 1):

$$q = \frac{4\pi}{\lambda} \times \sin\theta \tag{1}$$

where λ is the wavelength of the incident radiation, 2θ is the scattering angle and is half the angle through which the radiation is scattered.

The empirical method such as graphical method can be used to determine the intensity (I_{max}), position (q_{max}), and width of the SAXS peak at half maximum (Δq) as described by Yuryev et al. (2004). Or the data can be fitted to a power-law function that describes the SAXS peak and the underlying diffuse scattering at low q. A Gaussian/Lorentzian peak (or the combination thereof) can be used to fit the lamellar peak around 0.06 $Å^{-1}$ and a Gaussian peak for the second-order reflection peak around 0.13 $Å^{-1}$ (Lopez-Rubio et al., 2008b; Blazek and Gilbert, 2010) as exampled in Eqs. (2) and (3):

$$I(q) = I_{max}\left[1 + \left(\frac{2(q - q_{max})}{\Delta q}\right)^2\right]^{-1} + Pq^{-\alpha} \tag{2}$$

The first term in Eq. (2) is the Lorentz function, which describes the SAXS peak, while the second term is a power-law function to account for the underlying diffusing scattering and provides the slope of the SAXS curves represented on a logarithmic scale, where P is the prefactor and α is the power-law exponent (Chanvrier et al., 2007).

$$I(q) = B + Pq^{-\alpha} + \frac{A\sqrt{\ln 2}}{W\sqrt{\pi}/4}\exp\left(-\frac{4\ln 2(q - q_0)^2}{W^2}\right) \tag{3}$$

The first term B in Eq. (3) is the background; the second term is the power-law function, where P is the power-law prefactor and α is the power-law exponent; the third term is a Gaussian function, where A is the Gaussian peak area, W (nm^{-1}) is the full width at half maximum of the peak, and q_0 (nm^{-1}) is the peak center position (Yang et al., 2016).

In the case of a complete q range over which the distribution of distances between crystals is available, the SAXS data can be fitted to a two phase nonparticulate model plus a power-law function for the underlying diffuse scattering as presented in Eq. (4) (Lopez-Rubio et al., 2008b):

$$I(q) = Pq^{-\alpha} + \left[\frac{BX_c(1 - X_c)\varepsilon^3}{(1 + q^2\varepsilon^2)^2}\right] \tag{4}$$

The first term of the equation (Eq. (4)) is the power-law model, and the second term is the "two-phase nonparticulate system" model, where X_c is the degree of crystallinity (vary between 0 and 1), ε is the characteristic length of the system, and B is the prefactor that is proportional to the electron-density contrast of the crystalline and amorphous phases.

One of the characteristics of SAXS is that many properties of disordered system can be described by quantities that are proportional to a power of another quantity. Particularly, the intensity I of the SAXS is proportional to negative power of the scattering vector, which is often called "power-law scattering" (Schmidt, 1991). I_{max} generally depends upon the amount of the ordered semicrystalline structures and/or the differences in electron density between crystalline and amorphous lamellae within the starch granules. The peak area indicates the degree of lamellae ordering (Pikus, 2005), the peak width depends on the regularity of the lamellar arrangement within starch granule (Blazek and Gilbert, 2010). As mentioned previously, in the low-q region, the curves comply with a simple power-law equation, where the exponent α gives insight into the surface/mass fractal structure of the starch granules. Specifically, the mass fractal dimension ($0 < \alpha < 3$) is used as an indicator for compactness of the starch samples, whereas the surface fractal dimension ($3 < \alpha < 4$) is used to indicate the degree of smoothness of the scattering objects (Suzuki et al., 1997; Zhang et al., 2015).

Further analysis of the SAXS measurements can be performed using two types of methods to extract parameters from the SAXS data. The first method is based on direct least-squares fitting of the observed intensity profile, which attempts to fit the observed intensity profile with a model (such as a simple paracrystalline model), where the intensity profile calculated from the model is least-squares fitted to the observed intensity, and various parameters of the model are thus iteratively refined (Cameron and Donald, 1992; Wang et al., 2007). The second method is based on correlation and interface distribution functions using Fourier-transformed intensity profile (Blazek and Gilbert, 2011), where the intensity data are Fourier transformed and the lamellar morphology in terms of structural parameters (such as lamellar repeat distance, crystalline and amorphous layer thicknesses, the width of the transition layer, and electron-density contrast) can be obtained by interpreting the resulting Fourier-transformed one-dimensional correlation function (Schmidt-Rohr, 2007; Wang et al., 2007; Yang et al., 2016).

The information regarding changes in structural organization of starch during the preparation of RS under various processing conditions can also be provided by SAXS technique. During the processing of waxy corn and potato starch under

high hydrostatic pressure, the SAXS results by fitting the data to a power law plus a Gaussian function (Eq. (3)) showed that both SAXS peak areas (corresponding to the lamellar phase) decreased, indicating that the starch gelatinization increases with the increasing pressure (Yang et al., 2016). The lamellar peak also broadened and the power-law exponent increased in low q region as pressure increased. By employing the linear correlation function, it was found that the long-period length and the average thickness of amorphous layers decreased when the pressure increased for both of the waxy starches. According to Chanvrier et al. (2007), the SAXS results by fitting the data to a power-law plus Lorentzian function (Eq. (2)) of the native maize starch containing various amount of amylose showed the characteristic peak at $q \sim 0.07$ Å^{-1}, which corresponds to the typical ~9–10 nm lamellar repeat of starch architecture within the granule (thickness of crystalline plus amorphous regions of the lamella). Comparatively, the intensity of the lamellar peak for the ERS (prepared after extrusion and storage) was decreased, which confirms the decreased crystallinity determined by XRD. The formation of crystals was reflected by the appearance of a shoulder in the SAXS patterns extending over a broad q range, which suggests the molecular reorganization with the formation of a heterogeneous semicrystalline structure. Shamai et al. (2004) also reported that the peak at Bragg distance of ~9 nm could be no longer observed in the scattering patterns of the RS_3 samples, indicating a complete disruption of the granule structure during the RS_3 production.

By observing under SAXS, Shamai et al. (2004) and Zabar et al. (2008) found that B polymorph with lamellas arranged in long-range periodicity was the major morphology when amylose corn starch was processed and recrystallized at low temperature. Contrarily, a mixture of A and V polymorphs without defined periodicity was found in starch processed and recrystallized at high temperature. Shrestha et al. (2015) has reported the appearance of a peak at $q \sim 0.135$ Å^{-1} on the SAXS curve of RS from extruded maize starch, which corresponds to a Bragg distance of ~4.6 nm. The corresponded peak is relevant to the marked increase in double helix and crystallinity (to a lesser extent) along with digestion time which increases in intensity with subsequent enzyme digestion after 4 h. The 4.6 nm of a B-type double helices corresponds to ~13 glucan residues along the helix axis or about three double helices orthogonal to the helix axis. Similar feature has also been reported for RS from HAMS previously (Lopez-Rubio et al., 2007; Zabar et al., 2008). By fitting the power law plus the two phase nonparticulate model, Lopez-Rubio et al. (2008b) found that the original lamellar repeat of granular starch characterized by a peak at the semicrystalline region ($q \sim 0.7$ Å^{-1}) cannot be observed in the RS fractions isolated from retrograded HAMS, a broad peak extending over a wide q range is instead observed which can be correlated with the growth of crystals in an amorphous matrix. An increased intensity on the SAXS curves for RS indicating an increase in the molecular order is also observed during the enzymatic process. Additionally a displacement of the curve toward higher q values also occur which suggest the growth of new crystals between the existent ones, leading to a decrease in the intercrystallite distance. The small angle X-ray scattering of *Canna edulis Ker* RS at different digestion stages show that the intensities of SAXS curves and the integrated area increase with the increasing digestion time, suggesting an increase in molecular order with the hydrolysis of amorphous components leading to the relative increase of electron density of crystalline material and distribution width of crystalline lamellar during enzyme digestion (Zhang et al., 2010).

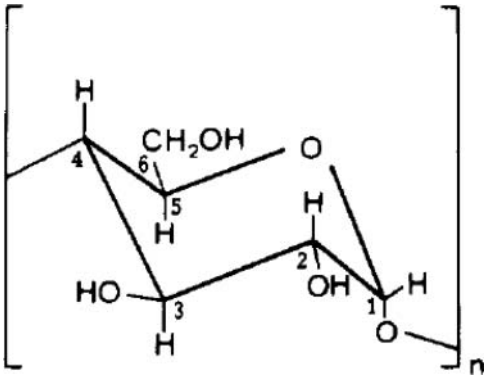

Figure 5. Starch molecule unit and the assignment of correspondent carbon numbers.

Measurement of structural conformation of RS by solid-state ^{13}C-NMR

The ^{13}C cross-polarization/magic angle spinning NMR (^{13}C CP/MAS NMR) is one of the emerging techniques that has been used for structural organization investigation of starch, based on the uniqueness of the C_1 resonance pattern by identifying the spectral frequencies by their chemical shift values. The spectral signals in different regions are assigned to carbon nuclei C_1-C_6 of α-1,4-D-glucan (Figure 5). Specifically, a carbon chemical shift for starch has been identified in 106–99 ppm for C_1; in 70–79 ppm for C_2, C_3, and C_5; in 80–84 ppm for C_4; and in 59–62 ppm for C_6. The conformational order of starch are directly correlated with the peak patterns of C_1 region which reveals the local electron densities characterized by glucosidic torsion angels on ^{13}C C/MAS spectra (Zhang et al., 2010). Therefore, the variations in C_1 multiplicity are often referred to show differences in the symmetry of double helix packing and crystallinity of RS by evaluating the intensity of C1 resonance. The relative degree of crystallinity of RS can be quantitatively estimated by the following equation (Eq. 5) (Zhang et al., 2014):

$$RC_L = S_F / S_T \times 100\% \quad (5)$$

where RC_L is the relative degree of crystallinity, S_F is the fitting peak area of C_1, and S_T is the total peak area of C_1.

In addition to providing information regarding the double-helical content in RS samples, the structural characteristics regarding the proportion of amorphous (single chain) and ordered (double helix) components inside the starch can also be estimated from ^{13}C CP/MAS spectra (Gidley and Bociek, 1985), which is comparable and complement to those results obtained from XRD pattern. The additional information on the linkage and the anomeric ring carbons in RS can also be

observed by ^{13}C-NMR spectral data. The two carbon nuclei C_1 and C_4, which are both involved in glycosidic linkages, are most sensitive for changes in polymer conformations and usually show large chemical-shift displacements between amorphous and crystalline materials. The ^{13}C-NMR spectroscopy results can also provide different information depending on the crystal polymorph. For example, in an A-type crystal polymorph, there are three peaks present at 102, 101, and 100 ppm; in a B-type polymorph, the C_1 resonance exhibits doublets (two peaks) at 101 and 100 ppm, which correspond to the non-identical sugar residues of amylose and amylopectin. The differences in C_1 resonance on ^{13}CNMR spectra for A and B crystal polymorphs could be attributed to the variation in their patterns of helices packing (Figure 3). Specifically, there is a twofold symmetry in an A-type structure and thus three different environments of C_1 sites with respect to adjacent double helices which is consistent with the observation of threefold multiplicity on the NMR spectra. Similarly, the threefold symmetry of adjacent helices is correspondent with the observed twofold multiplicity. The C_2, C_3, and C_5 regions mainly showed that the B-type double helices resulting from the residues of free amylose, whereas the C_4 region represents information on the amorphous domains. The appearance of two broad resonance peaks at 82 ppm for C_4 could arise from the amorphous state (Flores-Morales et al., 2012; Fan et al., 2013). According to Mahadevamma et al. (2003) and Gidley et al. (1995), the presence of doublet in the region 100–102 ppm was attributed to C_1 of the B-type crystalline polymorph of RS, such doublet region could not be observed in less crystalline starches. In a V-type crystal polymorph, a broad peak of C_1 at 193 or 104 ppm corresponds to a typical single helix organized in a V-type crystalline phase or dispersed in an amorphous phase (Baik et al., 2003; Thérien, 2007).

According to previous study, the results obtained from solid-state NMR and XRD data have some divergence. It was reported that the double helix content in native starch measured by NMR is considerably higher than the crystallinity determined from XRD (Gidley and Bociek, 1985; Cooke and Gidley, 1992). It is thus referred that the molecular-ordered regions containing double helices not involved in crystalline arrays are indeed present within the granule. Since unlike high-resolution solid-state NMR, XRD results only reveal the information regarding the repeating nature of double helical with negligence of irregularly packed structure. According to Shrestha et al. (2015), the difference between granular and extruded maize starches was observed in the relative extents of double-helical order obtained by the solid-state NMR and associated A- or B-type crystallinity obtained by XRD. The relative amounts of these two parameters were similar before and during digestion of granular starches, suggesting that most double helices were part of crystallites. However, the extruded samples exhibited much higher measured levels of double helices than crystallinity after extensive digestion treatment, indicating that many of the double helices that are either resistant from the start of digestion or formed during the digestion process are arranged in a relatively noncrystalline fashion, and yet are resistant to digestion. Mutungi et al. (2011) found that the NMR values of crystalline double helices were ~10% higher than the degree of crystallinity measured by XRD in the recrystallized cassava starch, indicating that some crystalline material is less repetitive or irregularly packed which thus was unable to diffract X-rays. The authors also found the difference between the NMR and XRD results in terms of the V-type (monohelical) glucosidic conformation which are not comparable due to low amounts presented.

According to Zhang et al. (2014), the lotus seed RS showed increased propensity for double helix formation and a higher relative crystallinity compared with those of native starch and HAMS according to ^{13}C NMR results, indicating that recrystallization was an important step to obtain a more stable structure during the formation of RS. Early studies found that the C_1 intensity for rice RS was relatively higher in the 99–102 ppm range and lower in the 93–99 and 102—106 ppm ranges, probably owing to the higher double-helical content in rice RS (Gidley and Bociek, 1988; Shukla, 1996). Mutungi et al. (2011) observed that the lack of resonance signal on the ^{13}C CP/MAS spectra at the C_4 site in the enzyme-isolated cassava RS, which could be due to removal of the amorphous conformations during digestion. The authors also found that C_1 resonances are generally broader although the positions of resonance peaks were retained, which signifies slight deviation from the glucosidic bond torsion angles distributions of highly homogeneous rigid conformation, leading to the formation of less rigid conformations due to enzyme-mediated disentanglement. Atichokudomchai et al. (2004) have proposed a proportion of C_4 peak fitting area relative to the total area of the spectrum method (C4-PPA method) to quantitative analyze the relative proportion of double helices, according to the authors, the amorphous phase decreased with the increase of double helix structure, whereas the proportion of the amorphous phase was related with the C4-PPA method. It was also demonstrated by Zhang et al. (2014) that the lotus seed RS (enzyme purified and freeze dried) has decreased total area of the spectrum on the ^{13}C-NMR spectrum, demonstrating a stable crystalline structure that involved with the formation of a higher proportion of double helix structure with the combination of amylose. The ^{13}C NMR results of resistant *Canna edulis* Ker starch (prepared by microwave heat-moisture treatment) obtained after 10 min and 18 h of digestion *in vitro* showed a doublet from B crystallites and three peaks from amorphous parts with C_1 atoms exhibit five peaks, suggesting that the spectrum could be assigned to combination of double-helical and amorphous polymorphs, and the validity of using C4-PPA method (Zhang et al., 2010).

Measurement of glycosidic linkage pattern of RS by permethylation and GC-MS

The glycosidic linkage pattern of RS derived from different botanical sources can be determined by GC-MS analysis, the preparation of appropriate derivatives yet is required prior to the application of GC-MS. A review has been given by Ruiz-Matute et al. (2010) regarding the derivation methods currently used for the analysis of carbohydrates by GC-MS. The permethylation followed by GC/MS analysis has been often used to analyze the glycosidic linkage composition of RS by converting sugars to partially O-methylated alditol acetates. The presence of peak on the GC/MS profile of 2,3,6-tri-O-methyl-D-glucose indicates a 1,4 linked

D-glucan backbone of RS. The identification of 2,3-di-O-methyl-D-glucose indicates the 1,6-branching presented in RS samples. The peak of 2,3,4,6-tetra-O-methyl-D-glucose identified on the GC-MS profiles is derived from the nonreducing moiety of RS molecule (Mahadevamma et al., 2003).

According to Mahadevamma et al. (2003), the results of permethylation followed by GC/MS analysis showed that the branched nature of purified RS derived from legumes having both 1,4 and 1,6 linkages, it was observed a structure reminiscent of amylopectin molecule (which has ~5% of branching) for RS from Bengal gram and red gram. Comparatively, Mangala et al. (1999a) found the purified RS from processed ragi to be a linear α-1,4-D-glucan, probably derived from a retrograded amylose fraction of ragi starch. A major peak of 2,3,6-tri-O-methyl D-glucose and minor peak of 2,3,4,6-tetra-O-methy D-glucose were identified, which are derived from the 1,4-chain-linked backbone glucose residues and the nonreducing glucose moiety. Almost comparable data were obtained both for ragi amylose and RS, suggesting that the latter is indeed derived from the former. Similar results were reported by Mangala and Tharanathan (1999) and Tharanathan and Tharanathan (2001) for RS derived from processed (autoclaved) rice and wheat with structure comprised essentially of linear α-1,4-D-glucan. The research conducted by Cairns et al. (1996) showed that the RS isolated from both pea amylose and pea starch gels was almost entirely composed of linear amylose chains and having a branched material comprising 0.7% enzyme resistant residue from the hydrolyzed amylose gel and 2.2% of the residue from the hydrolyzed starch gel. It was also observed that the methylation analysis of enzyme resistant residues from chickpea gel and *in vivo* RS recovered from the ileostomy effluent showed somewhat a higher proportion of branched materials (i.e., with values of 4.2 and 5.5%, respectively).

The structural modification of type-4 RS from amylose and amylopectin caused by dry heating was studied by Nunes et al. (2016) by methylation and GC analysis, it was observed that the decrease of 1→4-linked Glc detected by methylation analysis after dry heating for polysaccharides and oligosaccharides samples can have a contribution of 1,6-anhydroglucose resides formed at the end of reducing end, it was thus concluded that the resistance to *in vitro* digestion seems to be due to the formation of new glycosidic linkages, different from the characteristics α-1,4 and α-1,6 of these polysaccharides.

Measurement of molecular order of RS by FT-IR

The FT-IR has been shown to be sensitive to changes in chain conformation, helicity, and double-helical structure (Goodfellow and Wilson, 1990), which thus can be used to provide useful information on the short-range molecular order (i.e., amorphous and crystallinity regions) of starch and confirms the long-range molecular-order results obtained from XRD. The RS samples are usually scanned in the wavenumber interval of 400–4000 cm^{-1} with background spectrum recorded using the solvent dissolved the RS sample (van Soest et al., 1995). By assigning and matching the band absorbance on FT-IR spectra with the vibrational modes of different chemical bonds based on empirical data, the variations in peak intensity could be used to suggest the occurrence of conformational changes in starch structure due to modifications in chain length, range ordering, and crystallinity, whereas the changes of amplitude in absorption bands on FT-IR spectra could be used to indicate more precise combination of internal and intermolecular hydrogen bonding during the RS formation. Generally no variations in chemical groups on FT-IR spectra are observed for RS derived from various origins when compared with their native starch.

Table 3. Band assignment for infrared spectra of starch and RS.

IR band (cm^{-1})	Band assignment
3100–3700	OH groups (O-H bond stretching)
2800–3000	CH_2 groups (C-H bond stretching)
~2930	O-H groups and CH_2 deformations
1743	C=O stretching vibration in a carboxyl group
1638	(COO–) stretching vibration in a carboxylate group
1600	carboxylate ion (COO)
1500	skeletal mode vibration of α-1,4 glycosidic linkage (C-O-C)
1300–1350	C-O-H, C-C-H, and C-O-H bending
1155, 1125, and 1105	C-O, C-C stretching with some C-OH contributions
1150 and 1080	coupling of C-O, C-C, and O-H bond stretching, bending, and asymmetric stretching of the C-O-C glycosidic bridge
1082, 1047, 1022, 995, and 928	C-O-H bending vibrations and CH_2-related modes
1022	characteristic of amorphous or disorder phase
995 and 1047	molecular order and crystallinity region of starch polymers
930 and 860	C-H bending
860	C-O-C symmetrical stretching and C-H deformation
620–527	skeletal modes of pyranose ring

Note: Summarized from van Soest et al. (1995), Capron et al. (2007), Lopez-Rubio et al. (2008a), García-Rosas et al. (2009), and Htoon et al. (2009).

The infrared spectroscopy is sensitive to the oscillatory frequencies of chemical bonds, and vibrational modes corresponding to the conformational and crystalline order of starch with generated absorption bands at different wavenumbers (cm^{-1}). The band assignments for infrared spectra in the region of 500–4000 cm^{-1} of starch and RS are summarized in Table 3. The FTIR spectrum is sensitive to changes of starch conformation and process of hydration, especially in the range of 1300–900 cm^{-1}, which generally reflects the C-C, C-OH, and C-H stretching vibration (van Soest et al., 1995). In particular, the band peaks at ~995 and ~1047 cm^{-1} corresponds to molecular order and crystallinity of starch polymers, their intensity increases as crystallinity of starch increases. Indeed the band 1047 cm^{-1} is consisted of two overlapping bands, which are positioned at 1040 and 1053 cm^{-1}. During starch molecule's reassociation, the 1040 cm^{-1} band appears very quickly, yet the 1053 cm^{-1} band requires a longer time to form. On the other hand, the vibrational modes resulting in the band intensity at ~1022 cm^{-1} are related to the amorphous or disorder phase, the intensity reduction of the peak at 1022 cm^{-1} is characterized as a reduction of crystallinity of starch (van Soest et al., 1995; Zhou et al., 2013). However in most cases, to allow compensation for vibration mode overlap effects, ratios of the integrated areas of absorption band at 1047/1022 and 995/1022

cm^{-1} are often used to quantify the degree of crystallinity and molecular order of the RSs. A higher ratio of 1047/1022 and 995/1022 cm^{-1} generally indicates a higher proportion of crystalline region in the starch granule. The ratio of intensity at 1047/1022 cm^{-1} could be used to characterize the degree of order, whereas the ratio of intensity at 995/1022 cm^{-1} could be used to descript the internal changes in the degree of double helix (Soest et al., 1995; Zhang et al., 2014).

According to Zhang et al. (2014) and Zeng et al. (2015), the absorption intensity of lotus seed RS in the band from 800 to 1200 cm^{-1}, which reflects C-C, C-OH, and C-H stretching vibration, was weaker than that of the native starch, indicating conformation changes occur in lotus seed RS. The authors also found that the ratio of absorbance at 995/1022 cm^{-1} was higher for RS (1.0) than that of native starch (0.87), suggesting the presence of microcrystalline are formed by the ordered starch chains. Zhou et al. (2013) also found that the RS from high-amylose starch had a higher ratio of 1047/1022 cm^{-1} compared with the starch before digestion. RS from thermal-treated starch, irrespective of moisture content, was of greater structural organization than RS from uncooked maize starch. Moreover, the starch molecules treated under higher moisture content tended to reorganize and then formed a more organized structure than starch treated under a lower moisture content based on the FT-IR observation. The changes in peak shapes and intensities in characteristic peaks at 1022 and 1047 cm^{-1} was observed for RS prepared from the retrograded tortillas starch (García-Rosas et al., 2009), implying a reduction in the amount of amorphous material due to retrogradation. As reported by Soest et al. (1995), the 995/1022 cm^{-1} ratio of lotus seed RS was significantly higher than the 1047/1022 cm^{-1} ratio, indicating the amount of double helices were higher than those of crystallinity, due to the assumption that not all of the double-helical structure were arranged into the crystal. The authors also found that the ultrasonic treatment of lotus seed starch promoted the formation of double helix, and microwave treatment had the weakest effect on enhancing the number of double helix structure.

According to García-Rosas et al. (2009), the -OH group band (~2930 cm^{-1}) was more pronounced in RS isolated from retrograded tortillas than the native starch, suggesting that the crystalline region increased with relatively high level of double-helical order in RS due to double helix formation with amorphous material either at the end of chains, in limited regions within helical chains, or trapped within aggregates, and the presence of a small amount of lipid complexes. It was found by García-Rosas et al. (2009) that the band at 1743 cm^{-1}, which represents for the C=O stretching vibration of carboxyl group, may also be related to the presence of Ca salts of carboxylic acids which are trapped in the double helix of retrograded starch. The carboxyl group band (i.e., peaks at 1743 cm^{-1}) was found to be more pronounced in RS compared to the control spectrum of maize starch, suggesting that the band area ratio increased for carboxylic groups in the RS. The variations in the IR region of 500–930 cm^{-1} was also found for RS derived from retrograded tortillas stored for 10 days compared with the raw starch, due to the structural modification on the skeletal modes of the pyranose (García-Rosas et al., 2009). Similar findings were also reported by van Soest et al. (1994) and Ogawa et al. (1998). According to Mahadevamma et al. (2003), the sharp appearance of peaks at 1653/1644 cm^{-1} for Bengal gram purified RS and 1653/1555 cm^{-1} for red gram purified RS in the IR spectra was due to –C=O absorption, with the formation of more numbers of potential reducing end groups in RS after the thermal modification of starch induced by reassociation of double helices of the amylose leached from the granule. As described previously, the alternation of the amplitude of absorption at other wavenumbers could also indicate the structural changes of the starch. Zhang et al. (2014) observed that the absorption band at 1367.22 cm^{-1} which corresponds to the bending vibration of $–CH_2OH$ (Table 3) for lotus seed RS was narrower than that of native starch. The amplitude of lotus RS in the absorption bands between 3100 and 3700 cm^{-1}(corresponding to the –OH group) was also found to be different from that of native starch, indicating the changes in the combination of hydrogen bonds generated during the formation of RS. For chemical modified RS_4, it was noticed that the appearance of absorbance at 1724 cm^{-1} which features the acetylated starch, corresponded to the stretching vibration of the C=O bond from the acetyl group (Chatel et al., 1997). Xie et al. (2006) also reported that a new peak occurs at 1724 cm^{-1} for chemical-modified RS_4, which was prepared by esterification of corn starch with citric acid. The absorption peak at 1746 cm^{-1} also was identified as the ester carbonyl group in bromoacetylated starch (Won et al., 1997) and octanoated starch (Aburto et al., 1997).

Measurement of molecular-weight and chain-length distributions of RS by HPSEC, GPC, HPAEC, and FACE

Differently from proteins which are genetically coded, starches are generally identified by their molecular-weight distribution, represented by the average molecular weights, number-average molecular weight (M_n), weight-average molecular weight (M_w), or z-average molecular weight (M_z). The M_w/M_n ratio represents for the value of the polydispersity index, the larger the value of the polydispersity index, the wider the molecular-weight distribution (Zhang et al., 2014). DP is the number of glucose units per polymer chain, as the molecular weight of glucose units is 162, the DP = M_w/162. HPSEC equipped with a refractive-index detector, GPCs coupled with refractive-index detector, HPAEC with pulsed amperometric detection, and FACE are common techniques used to measure the molecular-weight and polymer chain-length distributions of RS.

By using SEC coupled with multiangle light scattering and refractive index detector (Zeng et al., 2015), the molecular-weight distribution of purified lotus RS prepared by autoclaving, microwave-moisture, and ultrasonic autoclaving treatments show a fraction of 86.6–89.9% in the ranges lower than 2×10^4 g/mol. Comparatively, the range of molar mass from 2×10^4 to 3×10^4 only accounts for 5.6–7.3%, and less than 7% of molecules are distributed in the range higher than 3×10^4. The M_n and M_w values of RS are also lower than those of native starch, indicating that the native starch might have higher amylose content than other types of starch analyzed. According to Zeng et al. (2015), the M_w value of RS prepared by ultrasonic-autoclaving treatment is the highest (1.60×10^4 g/mol), whereas the RS prepared by autoclaving treatment has

the lowest M_w value (1.52×10^4 g/mol). Based on the measurement using HPSEC coupled with RI detector, the M_w of ragi (finger millet, *Eleusine coracana*) RS isolated by sequential enzymatic digestion and purified by GPC from the five-cycle-autoclaved finger millet flour is reported to be $\sim 1.4 \times 10^6$ Da. The value is similar to the M_w of RS derived from the *in vivo* which is the undigested starch fraction obtained from the ileum of rat intestine and is slightly less than that of ragi amylose ($\sim 1.6 \times 10^6$ Da) (Mangala et al., 1999a). Comparatively, the alkaline purified RS from five-cycle-autoclaved rice flour has a molecular weight of $\sim 1.2 \times 10^6$ Da, which constitutes 7400 D-glucose resides per molecule of RS (Mangala and Tharanathan, 1999).

The M_w/M_n (i.e., polydispersity index) of RS prepared by autoclaving, microwave-moisture, and ultrasonic-autoclaving treatments are between 1.247 and 1.298, indicating that RS samples have relatively narrow molecular-weight distribution (Zeng et al., 2015). Similar observation have been reported by Zhang et al. (2014) that the M_w/M_n ratio of lotus RS purified by different methods are in the range of 1.044–1.689, compared with that of unpurified lotus RS with a M_w/M_n ratio of 4.118, indicating that an overall orderly level of the starch molecules with stable double helix structure are formed during RS preparation. The molecular weight of the polymer is completely homogenous when the value of the polydispersity index is 1. The observation of the close to 1 ratio of M_w/M_n suggests that the lotus RS is degraded during RS preparation by autoclaving and then reformed molecular chains with a low DP which provide several chain ends where stable double-helical structure can be easily formed (Zhang et al., 2014).

The relatively appropriate DP is beneficial for the formation of double helices and crystallization (Luckett, 2012). Based on earlier studies, a minimum chain length of 30–40 glucose residues seems to be a requirement for the formation of RS. Longer chains promote RS formation whereas their complexing with lipid due to the helical conformation prevents the RS formation. The starch with B-type polymorph usually have lower percentages of short chains (DP of 6–12) and higher percentages of long chains (DP $\geq$ 37) than the A- and C-type polymorphs (Jane et al., 1999). The data of molecular weight or DP can be obtained by the intergradation of peaks which are considered as an assembly of many component DPs with cumulative weight fractions at different molar mass ranges on the HPSEC profile. The weight-average DP (DP_w) and number-average DP (DP_n) can be calculated from $DP_w = \sum(A_iM_i)/\sum A_i$ and $DP_n = \sum(A_i/A_i/M_i)$, respectively, where A_i is the peak area of the fraction I and M_i is its molecular weight. The polydispersity (p) is given by the ratio of DP_w/DP_n (Cairns et al., 1995).

With the coupling use of debranching enzymes such as isoamylase and pullulanase, the information of the chain-length distribution of RS can be obtained by HPSEC, HPAEC, and FACE. The FACE method, which is based on the attachment of fluorescent dyes to the reducing end of starch followed by high-resolution separation on polyacrylamide slab gels, can be used to determine the amylopectin chains. However, longer chains (DP > 100), including extra-long amylopectin and amylose chains cannot be detected by FACE, instead, can be determined by HPSEC. Although HPSEC has the disadvantages of band-broadening, calibration, and inaccuracies in the Mark-Houwink relation compared with FACE (Wu et al., 2014). To the best of author's knowledge, very little research has been done on the utilization of FACE to investigate the chain-length distribution of enzymatic RS. A detailed review of FACE method has been given by Starr et al. (1996) and Hu (1995). The branch chains can be categorized into the following four fractions: DP of 6–12, 13–24, 25–36, and $\geq$37 (Hanashiro et al., 1996). The long chains are mostly hydrolyzed into optimal-length chains due to entropic reasons which then acquire the capacity to form more stable enzyme resistant structure (Lopez-Rubio et al., 2008b). The complete alignment of longer polymers was destroyed, the too short chains were also absent in RS as they lack the minimum length for forming of stable double helices (Eerlingen et al., 1993b). Shrestha et al. (2015) found that the enzymatic RS fraction has an increased number of short branches (39% DP < 13) compared with the extruded maize and HAMS (25% DP < 13). The authors inferred that the short branch length amylopectin fragments, which are not capable of crystallizing, are most possibly attached to linear chain portions covalently and remain enzymatic resistance due to high level of molecular order. The FACE data for maize starch showed that the amylopectin branches resisting digestion had remarkably little difference up to 24 h of digestion, which are similar to those findings reported by Shrestha et al. (2015) that the branch-length distribution showed only minor changes during the course of digestion. Other researchers have also reported the DP_n values of 20–30 (Gidley et al., 1995), 19–26 (Eerlingen et al., 1993b), and 13–17 (Lopez-Rubio et al., 2008b) in RS isolated from recrystallized starch of different botanical origins. The analysis of RS recovered from the terminal ileum in humans showed that three populations of α-glucans are recovered by intubation or from ileostomy bags, i.e., low DP of 1–5, intermediate DP of 13–38, and high DP < 100 molecular weight (Faisant et al., 1993). The average DP_n value of about 35 glucose units was reported by Faisant et al. (1993) for the RS fraction isolated from the ileal terminus of the human small intestine following ingestion of retrograded starch. The RS prepared from the autoclaved wheat starch gels has chain lengths of around DP of 50 and 65, which was composed of linear α-glucans (Russell et al., 1989; Siljeström et al., 1989). According to Zeng et al. (2015), the DP values of RS prepared by autoclaving, microwave-moisture, and ultrasonic-autoclaving treatments are between 89 and 98. The HPSEC profile of the RS produced by *in vitro* hydrolysis of retrograded pea starch gels and pea amylose gels by porcine pancreatic α-amylase, show that the RS sample, consisting of semicrystalline, are mostly linear and are present in two main molecular size subfractions, i.e., (i) DP > 100 (composed of semicrystalline material present in the retrograded part of the gel) and (ii) DP of 20–30 (arising from recrystallized amylose fragments released during degradation by α-amylase). A third minor subfraction which is composed of oligosaccharides with DP $\leqq$ 5 is also found in the RS sample (Cairns et al., 1996). Mutungi et al. (2011) observed that the enzymatically-isolated cassava RS residues (prepared by debranching and recrystallization by annealing, temperature-cycle, or heat-moisture treatments) had higher DP between 22 and 23 than those of native and undigested recrystallized starch. The amount of longer chains (DP of 18–44) was also found to be higher in RS, suggesting that

linear polymers are capable of forming ~3–8 helical turns with more enzyme resistant structures. The polymer chains of DP of ~36 exhibited the highest digestible resistance activity. The formation of RS greatly depends on the processing conditions applied during their preparation. For example, the chain length of the retrograded amylose in the crystalline zones might be affected by conditions such as concentration, temperature, as well as hydrolytic reagent (enzymes) employed during the preparation and isolation of the RSs (Eerlingen et al., 1993b). The magnitude variations observed in DP values which represents for the changes in abundance of polymer chains, generally reflect the differences in enzyme hydrolysis kinetics of the starches.

The molecular composition of RS from uncooked and cooked high amylose starches (HAS) analyzed by HPSEC coupled with evaporative light scattering detector show differences in the ratio of amylopectin/amylose (Zhou et al., 2013). Specifically RS from uncooked HAS exhibited the highest amylopectin fraction in the molecular profile, followed by RS from nonmoisture thermal treatment, the amylopectin fraction is found to be absent in the molecular profile of RS from hydrothermal treatment, implying that the enzymatic susceptibility is greatly enhanced especially for amylopectin fraction under thermal treatment with or without moisture. According to Polesi and Sarmento (2011), the chickpea RS prepared by hydrolysis using acid coupling with heat treatment shows no amylopectin peak on the GPC profile, indicating that the amylopectin are hydrolyzed into lower molecular-weight chains. On the other hand, the chickpea RS prepared by hydrolysis using enzyme and heating treatment shows the presence of chains of more even M_w. In addition, the acid hydrolysis led to the largest reduction in M_w than the enzymatic hydrolysis, indicating that acid promotes an intense starch rupture.

The study conducted by Yin et al. (2007) found that the RS obtained from sago starch treated by pullulanase consists of fractions of low polymerization degree, with a small amount of remaining fraction with high M_w. A reduction of M_w is also observed in sago RS compared with the native starch. By using GPC coupled with differential refractive index detector (Cai et al., 2010), the M_w distribution shows that the RS produced from debranching of waxy maize starch have a relatively low DP which is further assembled into a highly crystalline structure, comparing with the long linear molecules of the high amylose starch. It suggested that the amylose chains are rearranged into enzyme resistant structure with higher crystallinity during the digestion process with alpha-amylase and glucoamylase. According to Chang and Moon (2015), the RS fraction isolated from heat-moisture treated waxy potato starch (HMT-RS), with a B-type X-ray pattern, show a higher proportion of long chains (DP $\geq$ 37) and a lower proportion of short branch chains (DP of 6–12) than the HMT potato starch and HMT-RS + SDS. Their observation indicated that the significant amount of short chains in amylopectin molecules interrupts the formation of crystallites resistant to enzymatic digestion during starch retrogradation, whereas amylopectin molecules with a small amount of short chains and large amount of long chains preferentially form relatively perfect crystallites resistant to digestion (Han et al., 2006; Chang and Moon, 2015).

Measurement of surface characteristics of RS by scanning electron microscopy and transmission electron microscopic

Unlike the SEM observation of native starch from different origins which generally shows the morphology of spherical-polygonal granules compactly packed in the endosperm cell walls (Figures 6a, 7a), the RS-rich powder tends to have irregular, rough, nonuniform morphology and their structures are relatively loose (Figures 6b, c; Figure 7b). Comparatively, the SEM images for enzyme purified RS from various botanical origins and/or prepared by different treatments generally feature a dense, compact, and sheet-like structure or gully shapes that is less smooth compared with the RS-rich power, due to the hydrolysis of amylose on the surface of the weak tissue structure with residues left (Figures 7c, d). The observation of SEM image generally supports the assumption of structural alternation during RS preparation and isolation processes, accompanied with the phenomenon of amylose leaching, loss of amylopectin crystalline region, and reassociation of starch chains within the starch granule. The compact structure maintained in RS as observed by SEM is probably due to the recrystallization of the gelatinized starch, with amylose and amylopectin molecules rearranged via hydrogen bonding by moving closer to one another, leading to the recomposition of the mixed-dimensional crystal beam and therefore maintaining the integrity of starch while at the same time increasing the degree of crystallinity of the RS. The correspondent changes reduced the action of enzymatic sties and enhanced its resistance to digestions.

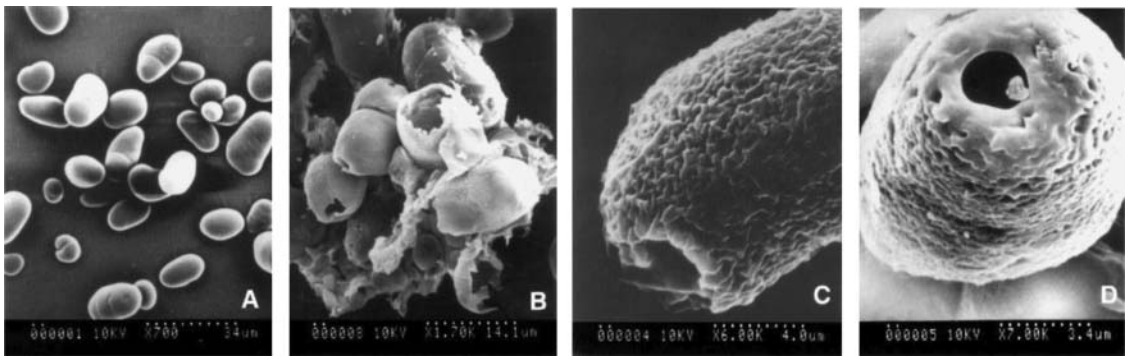

Figure 6. Scanning electron micrographs of: (a) native mung bean starch granules; (b)–(d) mung bean starch hydrolyzed (71.1%) by porcine pancreatic amylase. Reproduced with permission from Hoover and Zhou (2003).

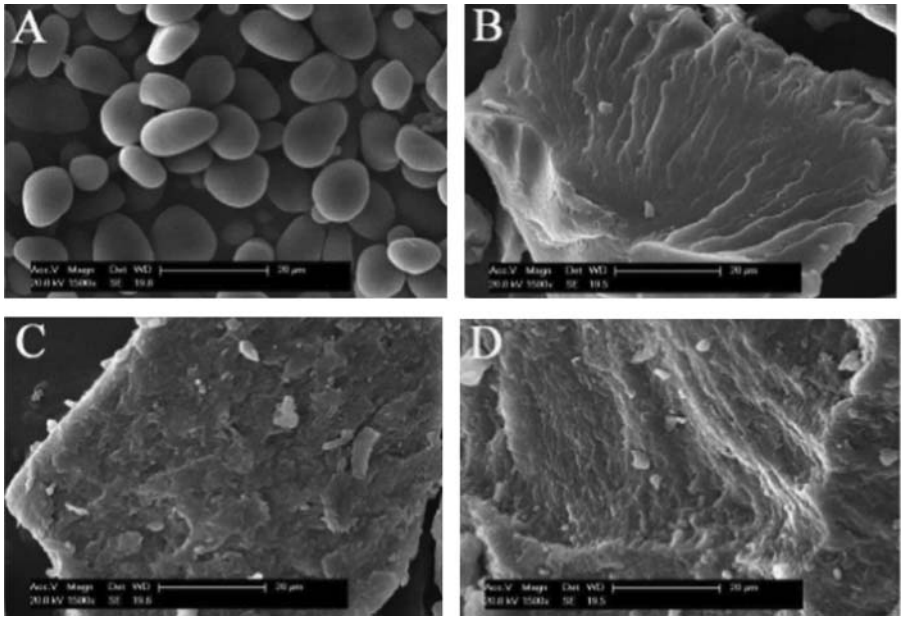

Figure 7. Scanning electronic micrographs of lotus seed native starch and lotus seed RS: (A) native starch; (B) unpurified lotus seed RS (NP-LRS3); (C) enzyme-purified lotus seed RS after drying (GP-LRS3); and (D) enzyme-purified lotus seed RS (ZP-LRS3). Reproduced with permission from Zhang et al. (2014).

As shown in the studies of Polesi and Sarmento (2011) and Miao et al. (2009), the granular structure generally disappears with the replacement of an amorphous mass of cohesive structure in isolated RS or RS-rich powders following different treatments including heating (boiling or repeated autoclaving), hydrolysis by acid or enzymes and retrogradation. Wang et al. (2014) examined the microscopic changes of banana RS during postharvest ripening, the results showed that compared with starch particles which had smooth surface during the initial ripening stages, RS tended to have starch particle surfaces rough and wrinkled during postharvest ripening due to the enzymatic effects. The SEM images for lotus seed RS showed that the original oval shape disappeared with the presence of a compact block structure compared with the smooth surface of the native starch granules. The presence of layered strips was also observed on the surface of lotus seed RS, in comparison with flaky and gully shapes noticed on the rough surface with more compact structure of enzyme-purified lotus RS (Zhang et al., 2014). Similar SEM images were reported for RS obtained from chickpea (Polesi and Sarmento, 2011) and corn (Kim et al., 2010).

The processing conditions and the intensity of the processing applied during the preparation of RS also have an influence on the microphotographs of RS. According to González-Soto et al. (2007), the RS rich samples prepared from autoclaved and debranched banana starch had a more compact structure when stored at 4°C for 24 h than those samples stored at higher temperatures, which could be attributed to higher level of cavities or channels in the matrix of starch stored at high temperature. The influence of storage temperature might also be due to the assumption that temperatures that are higher than the glass transition temperature (T_g) avoid the retrogradation phenomenon due to the movement of starch chains and lead to the appearance of a rubbery state. The fragmented, hollowed, and half-shell-like granules were observed in the RS residues of maize amylose-extender (ae) mutant starch (prepared by enzymatic hydrolysis of native ae-line starches at 95–100°C) (Jiang et al., 2010a), which was likely to be the remnants of the outer layer of spherical granules. It was thus inferred by the authors that the RS was more concentrated at the outer layer of the spherical starch granules or in role/filamentous starch granules. Moreover, starch molecules around the hilum were gelatinized and hydrolyzed rapidly since the starch molecules around the helium were loosely packed and contained less amylose. According to Sievert and Pomeranz (1989), the RS residue, isolated from the autoclaving-cooling treated sample, has disappeared porous structure, which is likely removed by the enzymatic treatment. The oven-dried RS residues tended to have very compact and dense formation compared with the vacuum-dried RS residue, which showed an open, fluffy structure with much higher melting enthalpy. The increased melting enthalpy could be ascribed to the better hydration capacity of vacuum-dried RS. According to Simsek and El (2012), the structure of taro RS (produced by autoclaving followed by debranching with pullulanase and retrogradation at room temperature) showed a continuous network and irregular shape with the disappearance of granule structure due to the occurrence of retrogradation. The density of the crystal structure thus greatly increased its resistance to enzyme attack.

The RS prepared by chemical modification yet somehow exhibited different SEM images. The SEM of RS_4 from normal and waxy corn starch appeared to have doughnut-shape with their outer sides drawn inwards (Figure 8), The area at the center of granule (i.e., hilum) was believed to be less organized than the rest of the granule as has been reported in corn starch enzyme and acid hydrolysis and cavitation originates at the hilum (Xie et al., 2006). The SEM results reported by Xie et al. (2006) and Xie and Liu (2004) suggested the chemical reagents such as citric acid could directly access a loosely organized

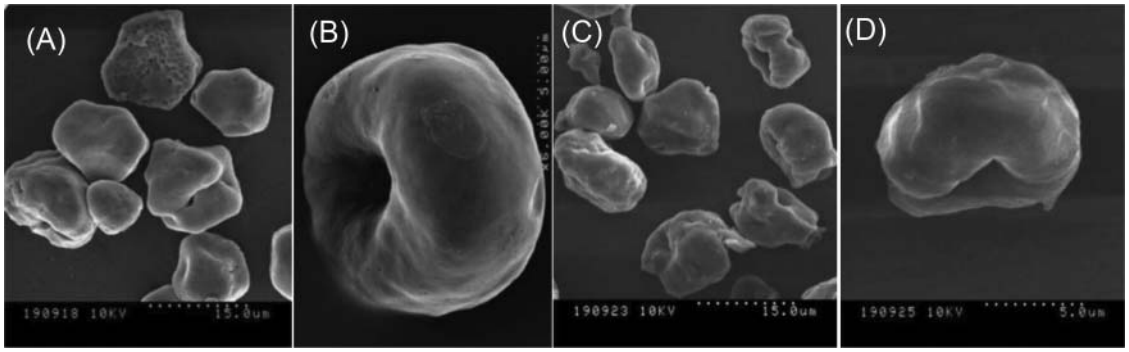

Figure 8. Scanning electron micrographs of normal corn RS (chemical cross-linking by citrate substitution) with RS content (78.8%) and degree of substitution (0.12), 2*k*; (b) normal corn RS (chemical cross-linking by citrate substitution) with RS content (78.8%) and degree of substitution (0.12), 6*k*; (c) waxy corn RS (chemical cross-linking by citrate substitution) with RS content (87.5%) and degree of substitution (0.16), 2*k*; (d) waxy corn RS (chemical cross-linking by citrate substitution), 6*k*; $k = 1000 \times$ magnification. Reproduced with permission from Xie et al. (2006).

region in the center of starch by channels and cavities, leading to an alteration in the granule morphology. The results of their study also indicated that the production of RS_4 by citrate substitution could prevent granular swelling and gelatinization. In another saying, the cross-linking by citrate substitution preserves granule structure during heating in water.

The detailed ultrastructure of RS produced by hydrolysis with α-amylase was studied using TEM by Pohu et al. (2004). The origin of the limited α-amylolysis of the RS products was explained by studying the two model substrates, waxy maize starch nanocrystals obtained by acid hydrolysis and A-type amylose crystals prepared from a low-DP amylose. The crystal structure of both substrates is presented as the association of double helices formed by DP of 15 amylose-like chains. The low DP crystals are formed by stacks of lamellae whereas lintners correspond to individual platelets. The results of TEM suggested that RS aggregates are resulted from the epitaxial growth of elementary crystalline A-type platelets. The authors proposed that the hydrolysis of RS occur on the side of the double helices instead of at their ends present at the surface of the lamellar crystals.

Measurement of structural order of RS by DSC

The DSC measurement provides us useful information on order-disorder transition processes of granular starch, by monitoring its changes in physical or chemical properties as a function of temperature by detecting the heat changes associated with such process. A peak is recorded on the DSC thermogram when changes occur in the differential heat flow that is associated with absorption or evolution of heat and could be used to reflect differences in associative bonding between polymer molecules. The area under the peak is directly proportional to the enthalpic change and its direction determines whether the thermal event is endothermic or exothermic (Biliaderis, 1983). The overall thermal characteristics are also dependent on water content, as water may exert a plasticizing effect and result in a decrease in T_g and increase in ΔH values (Mahadevamma et al., 2003). Together with XRD methods, DSC is another probe of structural order of RS by revealing their thermodynamic properties. The melt transition of RS from solid to the fluid state can be described as dissociation of ordered regions composed of double-helical segments and double helix to single coil transitions (Sievert and Wursch, 1993). The DSC thermal responses are also directly related to the number of helices present, regardless of their tertiary organization (Sievert et al., 1991).

The variations of DSC data for RS including their gelatinization temperatures, enthalpy and heat capacity changes, as observed in Table 4, reflect the differences in their degrees of crystallinity and intermolecular bonding, which are in turn influenced by the genotypic factors for RS from different food sources as well as different processing conditions applied during RS preparation. In normal cases, the retrograded amylopectin mostly melts in the approximate temperature range of 40–70°C, whereas retrograded amylose melts at higher temperatures, from 120 to 170°C (Sievert et al., 1991). The presence of long-chain double-helical crystallites of amylose is responsible for its high gelatinization temperature which facilitates the formation of elongated starch granules (Jiang et al., 2010b).

The study carried out by Sievert and Pomeranz (1989) showed that the heat-moisture-treated amylomaize starch (RS-rich powder) exhibited the endothermic transition temperature in the range between 120 and 165°C, due to dissociation of crystalline amylose (Table 4). The isolated RS samples, however, exhibited sharper endotherms over a broader temperature range with higher melting enthalpies, as the enzymatic treatment removes the degradable starch. Contrarily, according to Haralampu (2001), the DSC profile of the retrograded amylose shows thermal activity from 100 to 165°C, depending on the M_w and how the amylose was retrograded (time/temperatures), whereas RS sample have peak temperatures ranging from 120 to 165°C on the thermogram and are associated with the melting of amylose double helices. Mutungi et al. (2011) have found that the recrystallized cassava RS prepared by annealing after digestion showed higher transition peak temperature compared with those before digestion, implying that RS sample existed in a more cohesive state.

The DSC enthalpy changes (ΔH) are generally considered to correspond to order-disorder transitions of crystallites (i.e., helices present in extended ordered arrays) and regions of lesser crystalline order. ΔH reflects the amount order, i.e., the enthalpy of melting of crystallites and double helices (Karim et al., 2000). According to Onyango et al. (2006), the endothermic enthalpies (0.2–1.6 J/g) associated with transition of RS_3 obtained from cassava starch were significantly

Table 4. The differential scanning calorimetric (DSC) data for RS from various botanical sources and prepared by different processing conditions.

RS sources	Processing methods of RS samples	DSC data					References
		T_o (°C)	T_p (°C)	T_c (°C)	ΔT (T_c-T_o)	ΔH (Cal g^{-1})	
Bengal gram	RS was prepared by pressure cooking followed by refrigeration cooling (four cycles), was isolated and purified by $HClO_4$ solubilization followed by GPC on precalibrated sepharose	61.1	63.2	73.5	12.4	1.53	(Mahadevamma et al., 2003)
Red gram *dhals*	Same as above	45.2	67.2	73.5	28.3	0.68	(Mahadevamma et al., 2003)
Rice (*Oryza sativa*, Intan variety)	RS was prepared from five-cycle-autoclaved rice, isolated by hydrolysis with termamyl, protease, and amyloglucosidase, and purified by HPSEC	94.7	106.1	118.2	23.5	1.58	(Mangala and Tharanathan, 1999)
Maize tortillas stored for 5 days	RS was isolated from tortillas starch by removing digestible starch with heat stable α-amylase, protease, and amyloglucosidase	23.4 (peak I)	31.9 (peak I)	45.4 (peak I)	13.5 (peak I)	7.1 (peak I)	(García-Rosas et al., 2009)
		131.6 (peak II)	139.7 (peak II)	149.5 (peak II)	9.8 (peak II)	3.6 (peak II)	
Maize tortillas stored for 10 days	Same as above	43.6 (peak I)	47.9 (peak I)	60.0 (peak I)	12.1 (peak I)	9.5 (peak I)	(García-Rosas et al., 2009)
		129.5(peak II)	146.8 (peak II)	169.3 (peak II)	22.5 (peak II)	24.6 (peak II)	
Cassava starch	RS was prepared with recrystallized starch prepared by annealing (ANN-DS) and digestion	—	—	—	69.72	37.43	(Mutungi et al., 2011)
	Temperature cycling (TC-DS) and digestion				68.15	33.07	
	heat-moisture treatment (HMT-DS) and digestion				70.31	50.28	
Maize amylose-extender (ae) mutant starch	RS was prepared by enzymatic hydrolysis of native ae-line starches at 95–100°C	100.7–107.7	118.6–121.4	139.7–158.8	—	12.2–25.7	(Jiang et al., 2010a)
Amylomaize starch	RS was prepared by repeated cycles (one to four) of autoclaving (121,134, and 148°C) and cooling overnight at 4°C; RS was isolated by treating with heat stable α-amylase (termamyl) at 100°C and amyloglucosidase at 60°C for 30 min, respectively, and dried either overnight at 105°C or vacuum dried.	120.9–125.9	152.5–153.6	162.0–166.4	—	8.2–19.7	(Sievert and Pomeranz, 1989)

Note: T_o is the onset temperature; T_p is the peak temperature, T_c is the conclusion temperature; ΔH is the enthalpy, and ΔT is the differential temperature.

lower than those of RS from cereals (25–30 J/g), it was assumed that RS_3 from cassava starch had few hydrogen-bonding linkages between the recrystallized amylose polymers and thus were structurally unstable and required less energy to dissociate. Compared with the native starch, the RS from debranched waxy rice starch generally exhibited higher peak melting temperature and endothermic enthalpy. Such behavior has been attributed to increased ordering and stabilization of double-helical structure through hydrogen bonds and other intermolecular forces, which consequently increased the degree of crystallite and stabilized the double-helical structure. Jiang et al. (2010a) also observed significantly higher gelatinization temperatures of RS residues prepared by enzymatic hydrolysis of maize amylose extender mutant starches than the native starch counterparts. The high onset gelatinization temperatures of RS residues implied the presence of long-chain double-helical crystallites which remained semicrystalline structures after heating at 95–100°C and enzymatic hydrolysis. The melting temperature range ΔT (i.e., T_c-T_o) can be used to interpret as a measure of the homogeneity of crystalline and noncrystalline conformation. Table 4 lists ΔT values of RS reported in previous studies, where the increase in T_c-T_o can be explained by a broader range of ordered arrays involving longer chains as implied by the relocation of T_c to higher temperature, and a more independent melting of individual crystallites and double helices subsequent to hydrolysis of amorphous phase. The higher enthalpies further indicate the formation of higher molecular order as a result of removal of disordered arrangements during digestion (Mutungi et al., 2011).

The endothermic multiplicity suggests the crystalline inhomogeneity, resulted from the presence of crystals with varying molecular stability. These phenomena could be generated from the wide range of glucan chain lengths present in starch, as a probable disordered intermingling of the different size glucans creating crystallographic defects of varying intensities within individual crystallites. According to Mahadevamma et al. (2003), the Bengal gram purified RS (by GPC) showed the first endothermic peak at 63.2°C and two sharp minor endotherms at around 99.7 and 96.2°C. The first peak could be attributed to the unmodified starch having a random coil amylose in retrograded crystallites. The endothermic peak were generally broad whereas the enthalpy values varied due to the overall gelatinization process, which was influenced by the associated polymeric constituents, and also decreases the net content of starch per se. Two endothermic peaks of RS observed on the DSC profile represents for two distinct populations of crystalline domains induced by the high-temperature cycling regime during

preparation of RS (Mutungi et al., 2011). According to García-Rosas et al. (2009), two peaks were observed for isolated RS sample in maize tortillas, the first endothermic transition (31.9–47.9°C) are indicative of amylopectin retrogradation endotherm during storage of tortillas sample (Table 4), which was at a temperature below gelatinization range, due to the reorientation or reassociation of the amylopectin branch chains into a less structural order in isolated RS than the one existing in the native starch. The gelatinization enthalpy also increased over time in tortillas (Table 4), attributed to the occurrence of more extensive retrogradation in tortillas over storage time. The second peak of transition occurred from 139.7 to 146.8°C which was caused by RS formation from amylose retrogradation. The increase in enthalpy of RS samples was also observed which could be due to increased number of hydrogen bonds than had to be broken before occurrence of RS swelling. Four types of endothermal peaks were observed by Polesi and Sarmento (2011) for chickpea RS prepared by hydrolysis and heat treatments, some samples exhibited one, two, or three peaks after the application of different treatments, where endotherm I (46–62°C) represents for the melting of retrograded amylopectin crystals (i.e., the melting of double helix short-chain structure), endotherms II–IV (131–171°C) was attributed to the melting of retrograded amylose crystals, which represents for the transition endotherms of the RS formed by long-chain glucans. According to Mangala et al. (1999a), the purified ragi RS from five-cycle-autoclaved rice showed endothermic peak between 100 and 104°C, as also have been reported for a few other cereal RSs in other studies (Gidley and Bociek, 1988). The enthalpy for the purified RS was 7.86 mcal mg^{-1} and for ragi RS enthalpy was 9.86 mcal mg^{-1}. Mangala and Tharanathan (1999) also observed the purified rice RS showed a broad endothermic peak staring at 80°C, and reaching a maximum at 110°C, with relatively low-enthalpy value of 1.58 mcal mg^{-1} (Table 4).

Research advances on relationship of structure and physiological effects of resistant starch

RS have shown to have a variety of health benefits including lowering postprandial plasma-glucose and insulin responses which could lead to increased insulin sensitivity and be beneficial for preventing type-2 diabetes. Apart from a direct impact on glycaemic response, most health benefits of RS could be attributed to its fermentation by the colonic microbiota, by producing SCFA by probiotics and makes an environment less liable to the development of cancerous tumors and contributes to the improvement of colon health (Robertson et al., 2000; Yao et al., 2009; Ai, 2013). The SCFA generated principally include acetate, propionate, butyrate and lactate, and gases like H_2, CO_2, and CH_4 (Cummings and Englyst, 1991). Butyrate is considered to play an important role in suppressing tumor cells and decreasing the proliferation of colonic mucosal cells; propionate may be involved in control of hepatic cholesterol synthesis, and also have been shown to stimulate large bowl epithelial proliferation, which may help maintain epithelial integrity. The acetic, propionic, and butyric acid can lower the lumen pH, leading to an acidic environment which could promote the healthy bacterial proliferation whereas inhibit pathogenic bacterial (Sharma et al., 2008). Other beneficial properties of RS consumption include the prevention of constipation, increasing excretion frequency and fecal bulk, decreasing production of mutagenic compounds and lowering the colonic pH and ammonia levels as well as the improvement of serum lipid profile and preventing obesity.

Substantial studies have been done on the structural characterizations of RS as comprehensively reviewed in the previous section. However, limited research has been carried out on investigating the relationship of structure and the corresponded physiological effects of RS. The chemical and physical structures of RS could greatly affect the rate and extent of fermentation, and the profile of the SCFAs formed. Schmiedl et al. (2000) and Dongowski et al. (2005) proposed that the RS_3 with a higher proportion of type-A crystallites has a poorer fermentation properties with slower degradation rate and lower quantities of SCFA and butyrate produced by bacteria, comparatively RS_3 with only B-type crystallites shows the superior fermentation ability with higher SCFA and butyrate levels obtained. Specifically, high concentrations and relatively high recrystallization temperatures (about 25°C) favor the formation of heat-stable RS with T_o and T_p values >110°C, could led to *in vitro* SCFA levels of 2000–2500 μmol/g faces (dry weight) with butyrate content of 30–60 mol%. The prebiotic properties of RS_3 rise with the increase in B-type microcrystalline filaments, which are also determined by this optimal composition of glucan chain length. The RS_3 stability, which is partially correlated to the crystallinity of the molecule, was enhanced with a higher proportion of chain length with 10–35 glucose units in the gel (Dongowski et al., 2005). As reviewed in the previous section, the differences in polymorphism types A and B could be ascribed to the chain lengths of the branch-chain double helices and the packing of the double helices in the RS structure. According to Lesmes et al. (2008), the possible effects of type-III RS crystalline polymorphism (type-A and -B patterns based on XRD study) on RS fermentability was also explored by human colonic microbiota and the short fatty acids production *in vitro*. The results of human fecal pH-controlled batch cultures suggested that changes in RS polymorphism could induce an ecological shift in the colonic microbiota and RS polymorph B may promote large bowel health. Specifically, RS_3 with polymorph B induced *Bifidobacterium* spp. and polymorph A induced *Atopobium* spp. In addition, RS_3 with polymorph B has been proved to help maintain higher *Bifidobacteria* in the proximal part of the colon and double their relative proportion in microbiota in the distal colon along with lowered total counts. Polymorph B also induced higher butyrate production to levels of 0.79 mM. The studies by Lesmes et al. (2008) has proposed the possibility of using different thermal processing treatments that resulting in different crystalline polymorphs of RS_3 to describe differences in the prebiotic capabilities of RS, especially its butryrogenicity in the human colon. Therefore, the parameters during the preparation of RS including temperature, polyglucan concentration in the gel, polymer chain-length distribution could be manipulated to control the effectiveness of butyrate formation, targeting for the promising utilization of RS in high-quality health-promoting functional food products.

By using a static anaerobic *in vitro* system, Zhou et al. (2013) has proved that the molecular structure of RS is one of the key

factors that determine SCFA production. According to HPSEC profile and SCFA and lactate analyses after *in vitro* fermentation by human gut bacteria, the results suggested that RS with larger molecules (amylopectin fraction) favored greater butyrate production than those without amylopectin fraction which has lower butyrate production. It thus indicated that the production of RS under different gelatinization/retrogradation processes could be manipulated to modulate bacterial fermentation pattern, which could subsequently influence the metabolites of ferments. Han et al. (2009) investigated the retarding effect of heat treatment of RS fraction from soybean on retarding of bile acid transport *in vitro*, it was found that XRD pattern of RS from soybean was altered after heat treatment, which correspondingly affected the retarding effect on bile acid transportation, and ultimately affected the cholesterol metabolism. According to Lehmann et al. (2002), the *in vitro* fermentation of the high stable RS with peak temperatures of ~145°C on the DSC thermograms resulted in a molar ratio of acetate:propionate:butyrate of 49:17:34.

Dongowski et al. (2005) examined two structurally different RS_3 (including RS_A, a mixture of retrograded maltodextrins; and RS_B, a retrograded potato starch) with respect to their physiological effect such as resistance to digestion, fermentability, and their effects on the composition and turnover of bile acids in rats. The HPAEC profile showed that RS_A consisted of a mixture of linear and branched polymers with a higher DP (35–100) of degraded amylose and amylopectin compared with RS_B, which is composed of a linear fraction with low M_w polymers (with DP between 10 and 35 glucose units) together with branched high M_w polymers of degraded amylopectin (with DP between 35 and 100). The results proved a strong relation between structures of RS_3, SCFA production and microflora. By studying the prebiotic properties of two types of RS_3, it was found that RS_A which is more resistant than RS_B with higher portion of B-type crystallites, increased the rate of fermentation accompanied by a decrease pH in cecum, colon, and feces, indicating that the resistant structure of RS_A are more stable and favor the formation of both SCFA and butyrate. Schmiedl et al. (2000) also supported the assumption that the quality of RS_3 under varying preparation conditions may differ strongly in their structure of insoluble crystallites during the reassociation of linear regions of the polymers, which are responsible for the resistance against α-amylases. The authors found that the fermentation of RS with high levels of low M_w polymers leads to significantly higher butyrate levels compared with conventional RS prepared from retrograded amylose-rich starch. Contrarily, RS_2 is a much poorer source for bacterial fermentation compared with RS_3. The isolated α-amylase RS_2 and RS_3 have demonstrated to be differentiated in their fermentation behavior, due to the variations in chemical and physical structure, particularly the polymer chain distribution in the resistant residues. Lehmann et al. (2002) also found that RS_3 from banana has a higher fermentation rate with high portion of butyrate produced than the native RS_2, where the SCFA concentrations was between 370 and 1800 μmol/g (dry matter) using RS_2 as fermentation substrate compared with SCFA levels of 890–2100 μmol/g generated using RS_3 as substrate. Englyst and Cummings (1986) also reported similar findings on the lower utilization raw banana starch (RS_2). According to the studies conducted by Cummings et al. (1996) in 12 healthy volunteers who ate controlled diets for 15 days periods, RS_2 (RS granules) tended to prolong transit time, which is not seen with RS_3. Both RS_2 and RS_3 have laxative properties and increased faecal total SCFA excretion, where the consumption of RS_2 (from potato and banana) led to greater proportions of acetate in faeces and RS_3 (retrograded starch from wheat and maize) resulted in the production of more propionate. The significant differences in prebiotic behavior of RS have not only been found between different types of RSs, variations are also observed among the same type of RS derived from different botanical origins. According to the studies conducted by Ferguson et al. (2000), three types of RS_2 were prepared from potato starch, HAMS, and α-amylase-treated HAMS, respectively. Significant differences were observed among RS from different sources, even though they were all classified as RS_2, where potato starch had the greatest effect on in increasing the amounts of SCFAs in large intestine, whereas HAMS had the least. In addition, potato starch, unlike HAMS, enhanced the proportion of butyrate.

The chemical-modified starch (RS_4) has been reported to generate different glucose responses (Raben et al., 1997). The effect of two different test meals containing 1–2% acetylated potato starch and β-cyclodextrin enriched potato starch (2–3%), respectively, was studied in humans, and only the latter was observed to lower the glucose level. However, the β-cyclodextrin was more effective and was more related to its distal absorption in the intestine or to delayed gastric emptying. According to Schulz et al. (1993), some RS_2 have shown to improve the magnesium and calcium absorption by enhancing mineral solubility in the cecum and/or large intestine, which has not been seen in case of RS_3. The increased absorption was assumed to be due to increased hypertrophy of the cecal wall and cecal acidification due to enhanced fermentation in the distal parts of the digestive tract (Lopez et al., 2000). The underlying mechanism of RS that are responsible for the increased ileal absorption of minerals thus need to be further explored in future studies to elucidate the detailed RS structure-mineral absorption relationship.

The RS has been reported to play an important role in the reduction of postprandial blood glucose and insulinemic responses to food due to the inaccessibility of starch to digestive enzymes (α-amylase, isoamylase, and pullulanase) (Homayouni et al., 2014; Raigond et al., 2015). The overall digestibility of RS depends on the category and source of RS consumed which has been found to vary per individual (Sharma et al., 2008). The variability may be attributed to individual differences regarding enzymatic responses due to structural differentiations among RS from different sources and prepared by different processing conditions. The research carried out by Williamson et al. (1992) demonstrated that the pattern of enzyme attack depends on the crystal type, and that each enzyme has a specific mode of attack on each type of crystallinity even in chemically homogeneous spherulites of a single crystalline type. Specifically, the hydrolysis of B-type structure is slower than A-type by all enzymes, probably due to surface area effects. A type shows no discernible spherulitic structure after partial hydrolysis, whereas the B-type spherulites retain a large

amount of visible spherical structure. Large differences were also observed for crystallinity after the hydrolysis with different enzymes. Behall et al. (1988) clarified that the consumption of a specific starch structure as the predominant carbohydrate source would lead to varied results in adult's postprandial glucose and insulin. They found that amylose meal resulted in a significantly lower glucose peak at 30 min than did the amylopectin meal. In addition, the plasma insulin response was significantly lower at 30 and 60 min after the consumption of amylose than the amylopectin meal. Hospers et al. (1994) also observed the significantly lower postprandial levels of glucose and insulin in blood and rating of satiety for pastas containing high amount of amylose. The authors suggested that the extent to which the structure of starch determines the rise in glucose or insulin levels after a food is consumed has not been positively correlated. The previously reviewed findings indicate that RS with different structural characteristics could lead to different reactions on postprandial glycemic responses. However, there is currently a dearth of information on the structural-function relationship regarding the structure of RS versus the sustained plasma glucose levels. This part of research would provide useful information with great potential benefit to carbohydrate sensitive or diabetic individuals.

Conclusion and future direction

The increased awareness of consumers concerning relationship between food, lifestyle, and health has been one of the reasons for the popularity of the enormous research on RS, including their structural characterization, and potential physiological studies. RS can be found in natural food from different origins (known as RS_1 and RS_2), or they can also be prepared and formed by processing by physical, enzymatic, and chemical modifications (known as RS_3 and RS_4, and RS_5). In this article, the structural characterizations of RS by the meaning of several techniques including XRD, SAXS, ^{13}C-NMR, GC-MS, FT-IR, HPSEC, HPSEC, GPC, HPAEC, FACE, SEM, TEM, and DSC have been summarized. The comparison of the structural characteristics of RS from naturally containing botanical origins (such as legumes, maize, potato) or RS-enriched products prepared by the application of various processing methods (such as debranching treatment, heat-moisture/autoclaving coupling with debranching treatment, autoclaving, and chemical modification) are extensively reviewed. Nevertheless, divergence exists among different researchers in the aspects of experimental procedures including the process of RS isolation as well as the detection techniques of RS structure. This is a need to develop standard methodologies for the RS isolation procedure as well as for the measurement of structural characteristics of RS. This will enable a realistic comparison of structural characterization of RS derived from various sources prepared by different methods. There are still significant gaps in our knowledge as to which structural features are critical in governing the kinetics and the extent of starch digestion. For instance, the role of crystallinity during the digestion, and whether enzyme resistant structure from *in vitro* and *in vivo* studies are still present in the original food matrices or whether they are formed during digestion as well as how effective currently used *in vitro* digestion methods are in simulating the digestion RS based foods in humans. These questions present a challenge that requires a multidisciplinary approach combining various fields of expertise.

RS are classified into five types according to their specific enzymatic resistance mechanism. The categorization of RS into types 1–5, however, may have certain constraints as they may contribute to the assumption that there is homogeneity within a type and the differentiation among the types is straightforward (Thompson, 2000). Studies have also shown that ingestion of pasta (RS_1), high-amylose corn starch (RS_2), retrograded starch (RS_3), cross-linked starch (RS_4), octenyl uccinic starch (RS_4), and FFA-complexed high-amylose corn starch (RS_5) could result in significantly lower postprandial plasma-glucose and/or insulin responses to varying extents compared with their respective control starch (Ai, 2013). Other variations in physiological effects including the prebiotic properties, the turnover of bile acids as well as the ability of improving mineral absorption were also found among the five categories of RS as reviewed above due to the differences in their structural integrity (Sharma et al., 2008). However, the specific structural characteristics of the respective RS types and the physiological function-structure relationship are not yet fully understood. Further studies are needed to clarify this assumption with detailed structural characterization and categorization of RS in order to better understand the relationship between structural characteristics and physiological effects.

Up until now, studies are more focused on the impact of RS levels on their physiological behavior such as the ability of butyrate production and hypoglycaemic effects (Zhao and Yang, 2009; Shi and Gao, 2011; Simsek and El, 2012; Zhou et al., 2014; Arcila and Rose, 2015). The physiological effects of RS depend on both the degree of its resistance to enzymatic activity and to a high extent by its composition and structure during preparation. For instance, the hypocholesterolemic properties of RS has also been found as RS particularly affects lipid metabolism on total lipids, total cholesterol, low-density lipoproteins, high-density lipoproteins, very-low-density lipoproteins, intermediate-density lipoproteins, triglycerides and triglyceride-rich lipoproteins, which makes RS beneficial for cardiovascular health. However, there are still controversial argues regarding the role of RS in altering triglyceride and cholesterol levels. It was previously reported that not all types of RS are found beneficial to the cholesterol level in blood. Therefore, additional studies need to be planned to determine the effects of RS on lipid metabolism in humans as well as the correlations between the structural characteristics of RS and their role in altering triglyceride and serum cholesterol levels. As has been reviewed previously, the intensity of SCFA formation as a result of fermentation in large intestine is not determined by the resistance degree, but by its composition and properties (Bednar et al., 2001; Zhao and Yang, 2009). Although few studies have been attempted to correlate the structural characteristics of RS versus (i) SCFA production by fermentation of RS; (ii) growth of *Lactobacilli* and *Bifidobacteria*; and (iii) excretion rates of cholesterol and bile acids, the structure-function relationship study of RS done so far are nevertheless limited to the crystallinity type based on XRD pattern, or chain-length distribution according to HPAEC profile, or molecular-weight distribution based on HPSEC measurement, none of the studies have

been carried out to explore the correlation of detailed structural composition/conformation of RS and their relative physiological effect. Moreover, more in-depth studies are required to elucidate the structural differences between physiologically RS and enzymatic RS, as well as their differentiations in the corresponded physiological properties, since the degree of mastication of foods, transit time, physical inaccessibility, amylase concentration, and the presence of other food components could all influence the enzymatic hydrolysis of RS from the lower ileum in humans with ileostomy and contribute to the amount of RS that reaches to the terminal ileum.

To the best of author's knowledge, no studies have been done until now on exploring the relationship of RS structure and their hypoglycaemic effects, therefore, the need to establish the quantitative structure-function relationships between structural composition/conformation and *in vitro*/*in vivo* postprandial plasma glucose and insulin responses after the consumption of RS is also highlighted to enable a comprehensive assessment of structure-function relationship of RS, which would lead to the establishment of fundamental knowledge for the furtherance understanding and application of RS to be served as nutritional ingredient in the development of various food products. Future studies are also needed for preparing RS with specific health benefits such as RS consumption targeting at lowering the glycemic response, and/or improved colon health, and/or hypocholeterolemic effect, so that the optimal characteristics of RS for specific physiological effects can be predicted. By answering this question, a good understanding of RS with respect to its structure and physiological effects relationships should be clearly achieved.

Funding

This work was supported in part by National Natural Science Foundation of China (31501405), Fundamental Research Funds for the Central Universities of China (GK201702012, GK201601002), and Natural Science Basic Research Plan in Shaanxi Province of China (2015JQ3081). Financial support from Young Talent Fund of University Association for Science and Technology in Shaanxi, China (20160209) is also greatly appreciated.

References

Aburto, J., Thiebaud, S., Alric, I., Borredon, E., Bikiaris, D., Prinos, J. and Panayiotou, C. (1997). Properties of octanoated starch and its blends with polyethylene. *Carbohydr. Polym.* **34**(1):101–112.

Ai, Y. (2013). Structures, Properties, and Digestibility of Resistant Starch. Ph.D. thesis, Iowa State University.

Alexander, L. E. (1969). X-Ray Diffraction Methods in Polymer Science. New York: Wiley-Interscience.

Arcila, J. A. and Rose, D. J. (2015). Repeated cooking and freezing of whole wheat flour increases resistant starch with beneficial impacts on *in vitro* fecal fermentation properties. *J. Funct. Foods* **12**:230–236.

Ashwar, B. A., Gani, A., Shah, A., Wani, I. A. and Masoodi, F. A. (2015). Preparation, health benefits and applications of resistant starch–A review. *Starch - Stärke* **9**(2):555–559.

Atichokudomchai, N., Varavinit, S. and Chinachoti, P. (2004). A study of ordered structure in acid-modified tapioca starch by 13C CP/MAS solid-state NMR. *Carbohydr. Polym.* **58**(4):383–389.

Baghurst, P. A., Baghurst, K. and Record, S. (1996). Dietary fibre, non-starch polysaccharides and resistant starch: A review. *Food Australia* **48**(3):S3–S35.

Baik, M. Y., Dickinson, L. C. and Chinachoti, P. (2003). Solid-state 13C CP/MAS NMR studies on aging of starch in white bread. *J. Agric. Food Chem.* **51**(5):1242–1248.

Bednar, G. E., Patil, A. R., Murray, S. M., Grieshop, C. M., Merchen, N. R. and Fahey, G. C. (2001). Starch and fiber fractions in selected food and feed ingredients affect their small intestinal digestibility and fermentability and their large bowel fermentability *in vitro* in a canine model. *J. Nutr.* **131**(2):276–286.

Behall, K. M., Scholfield, D. J. and Canary, J. (1988). Effect of starch structure on glucose and insulin responses in adults. *Am. J. Clin. Nutr.* **47**(3):428–432.

Biliaderis, C. G. (1983). Differential scanning calorimetry in food research–A review. *Food Chem.* **10**(4):239–265.

Blazek, J. and Gilbert, E. P. (2010). Effect of enzymatic hydrolysis on native starch granule structure. *Biomacromolecules* **11**(12):3275–3289.

Blazek, J. and Gilbert, E. P. (2011). Application of small-angle X-ray and neutron scattering techniques to the characterisation of starch structure: A review. *Carbohydr. Polym.* **85**(2):281–293.

Buléon, A., Colonna, P., Planchot, V. and Ball, S. (1998). Starch granules: Structure and biosynthesis. *Int. J. Biol. Macromol.* **23**(2):85–112.

Cairns, P., Morris, V., Botham, R. and Ring, S. (1996). Physicochemical studies on resistant tarch *in vitro* and *in vivo*. *J. Cereal Sci.* **23**(3):265–275.

Cairns, P., Sun, L., Morris, V. and Ring, S. (1995). Physicochemical studies using amylose as an *in vitro* model for resistant starch. *J. Cereal Sci.* **21**(1):37–47.

Cai, L., Shi, Y. C., Rong, L. and Hsiao, B. S. (2010). Debranching and crystallization of waxy maize starch in relation to enzyme digestibility. *Carbohydr. Polym.* **81**(2):385–393.

Cameron, R. and Donald, A. (1992). Small-angle X-ray scattering study of the annealing and gelatinization of starch. *Polymer* **33**(12):2628–2635.

Cao, J., Billows, C. A., Cao, J. and Billows, C. A. (1999). Crystallinity determination of native and stretched wool by X-ray diffraction. *Polymer Int.* **48**(48):1027–1033.

Capron, I., Robert, P., Colonna, P., Brogly, M. and Planchot, V. (2007). Starch in rubbery and glassy states by FTIR spectroscopy. *Carbohydr. Polym.* **68**(2):249–259.

Chang, J. L. and Moon, T. W. (2015). Structural characteristics of slowly digestible starch and resistant starch isolated from heat-moisture treated waxy potato starch. *Carbohydr. Polym.* **125**:200–205.

Chanvrier, H., Uthayakumaran, S., Appelqvist, I. A., Gidley, M. J., Gilbert, E. P. and López-Rubio, A. (2007). Influence of storage conditions on the structure, thermal behavior, and formation of enzyme-resistant starch in extruded starches. *J. Agric. Food Chem.* **55**(24):9883–9890.

Charalampopoulos, D., Wang, R., Pandiella, S. and Webb, C. (2002). Application of cereals and cereal components in functional foods: A review. *Int. J. Food Microbiol.* **79**(1):131–141.

Chatel, S., Voirin, A. and Artaud, J. (1997). Starch identification and determination in sweetened fruit preparations. 2. Optimization of dialysis and gelatinization steps, infrared identification of starch chemical modifications. *J. Agric. Food Chem.* **45**(2):425–430.

Cheetham, N. W. and Tao, L. (1998). Variation in crystalline type with amylose content in maize starch granules: An X-ray powder diffraction study. *Carbohydr. Polym.* **36**(4):277–284.

Chiu, C. W., Henley, M. and Altieri, P. (1994). Process for making amylase resistant starch from high amylose starch. US Patent 5281276.

Cooke, D. and Gidley, M. J. (1992). Loss of crystalline and molecular order during starch gelatinisation: Origin of the enthalpic transition. *Carbohydr. Res.* **227**(0):103–112.

Cummings, J. H., Beatty, E. R., Kingman, S. M., Bingham, S. A. and Englyst, H. N. (1996). Digestion and physiological properties of resistant starch in the human large bowel. *Br. J. Nutr.* **75**(5):733–747.

Cummings, J. H. and Englyst, H. N. (1991). Measurement of starch fermentation in the human large intestine. *Can. J. Physiol. Pharmacol.* **69**(1):121–129.

DeVries, J. W. (2004). Dietary fiber: The influence of definition on analysis and regulation. *J. AOAC Int.* **87**(3):682–706.

Dongowski, G., Jacobasch, G. and Schmiedl, D. (2005). Structural stability and prebiotic properties of resistant starch type 3 increase bile acid turnover and lower secondary bile acid formation. *J. Agric. Food Chem.* **53**(23):9257–9267.

Eerlingen, R. C., Crombez, M. and Delcour, J. A. (1993a). Enzyme-Resistant starch. I. Quantitative and qualitative influence of incubation-time

and temperature of autoclaved starch on resistant starch formation. *Cereal Chem.* **70**(3):339–344.

Eerlingen, R.C, Deceuninck, M. and Delcour, J. A. (1993b). Enzyme-Resistant starch. II. Influence of amylose chain length on resistant starch formation. *Cereal Chem.* **70**(3):345–350.

Englyst, H. N. and Cummings, J. H. (1986). Digestion of the carbohydrates of banana (Musa paradisiaca sapientum) in the human small intestine. *Am. J. Clin. Nutr.* **44**(1):42–50.

Englyst, H. N. and Cummings, J. H. (1987). Resistant starch, a new food component: A classification of starch for nutritional purposes. In: Cereals in a European Context. First European Conference on Food Science and Technology, pp. 221–233. Morton, I. D. (Ed.). Chichester: Ellis Horwood.

Englyst, H. N., Kingman, S. and Cummings, J. (1992). Classification and measurement of nutritionally important starch fractions. *Eur. J. Clin. Nutr.* **46**:S33–S50.

Faisant, N., Champ, M., Colonna, P., Buleon, A., Molis, C., Langkilde, A., Schweizer, T., Flourie, B. and Galmiche, J. (1993). Structural features of resistant starch at the end of the human small intestine. *Eur. J. Clin. Nutr.* **47**(4):285–296.

Fan, D., Ma, W., Wang, L., Huang, J., Zhang, F., Zhao, J., Zhang, H. and Chen, W. (2013). Determining the effects of microwave heating on the ordered structures of rice starch by NMR. *Carbohydr. Polym.* **92** (2):1395–1401.

Faraj, A., Vasanthan, T. and Hoover, R. (2004). The effect of extrusion cooking on resistant starch formation in waxy and regular barley flours. *Food Res. Int.* **37**(5):517–525.

Ferguson, L. R., Tasman-Jones, C., Englyst, H. and Harris, P. J. (2000). Comparative effects of three resistant starch preparations on transit time and short-chain fatty acid production in rats. *Nutr. Cancer* **36** (2):230–237.

Flores-Morales, A., Jiménez-Estrada, M. and Mora-Escobedo, R. (2012). Determination of the structural changes by FT-IR, Raman, and CP/MAS 13 C NMR spectroscopy on retrograded starch of maize tortillas. *Carbohydr. Polym.* **87**(1):61–68.

Fuentes-Zaragoza, E., Sánchez-Zapata, E., Sendra, E., Sayas, E., Navarro, C., Fernández-López, J. and Pérez-Alvarez, J. A. (2011). Resistant starch as prebiotic: A review. *Starch-Stärke* **63**(7):406–415.

Gallant, D. J., Bouchet, B. and Baldwin, P. M. (1997). Microscopy of starch: Evidence of a new level of granule organization. *Carbohydr. Polym.* **32** (97):177–191.

García-Rosas, M., Bello-Pérez, A., Yee-Madeira, H., Ramos, G., Flores-Morales, A. and Mora-Escobedo, R. (2009). Resistant starch content and structural changes in maize (zea mays) tortillas during storage. *Starch - Stärke* **61**(7):414–421.

Gidley, M. J. (1987). Factors affecting the crystalline type (A–C) of native starches and model compounds: A rationalisation of observed effects in terms of polymorphic structures. *Carbohydr. Res.* **161**(2):301–304.

Gidley, M. J. and Bociek, S. M. (1985). Molecular organization in starches: A carbon 13 CP/MAS NMR study. *J. Am. Chem. Soc.* **107**(24):7040–7044.

Gidley, M. J. and Bociek, S. M. (1988). Carbon-13 CP/MAS NMR studies of amylose inclusion complexes, cyclodextrins, and the amorphous phase of starch granules: Relationships between glycosidic linkage conformation and solid-state carbon-13 chemical shifts. *J. Am. Chem. Soc.* **110**(12):3820–3829.

Gidley, M., Cooke, D., Darke, A., Hoffmann, R., Russell, A. and Greenwell, P. (1995). Molecular order and structure in enzyme-resistant retrograded starch. *Carbohydr. Polym.* **28**(1):23–31.

Godet, M. C., Bizot, H. and Buléon, A. (1995). Crystallization of amylose–Fatty acid complexes prepared with different amylose chain lengths. *Carbohydr. Polym.* **27**(1):47–52.

González-Soto, R., Mora-Escobedo, R., Hernández-Sánchez, H., Sanchez-Rivera, M. and Bello-Pérez, L. (2007). The influence of time and storage temperature on resistant starch formation from autoclaved debranched banana starch. *Food Res. Int.* **40**(2):304–310.

Goodfellow, B. J. and Wilson, R. H. (1990). A Fourier transform IR study of the gelation of amylose and amylopectin. *Biopolymers* **30**(13–14):1183–1189.

Han, X.-Z., Ao, Z., Janaswamy, S., Jane, J.-L., Chandrasekaran, R. and Hamaker, B. R. (2006). Development of a low glycemic maize starch: Preparation and characterization. *Biomacromolecules* **7** (4):1162–1168.

Hanashiro, I., Abe, J. I. and Hizukuri, S. (1996). A periodic distribution of the chain length of amylopectin as revealed by high-performance anion-exchange chromatography. *Carbohydr. Res.* **283** (10):151–159.

Han, S. H., Seog-Won, L. and Chul, R. (2009). Effect of heat treatment of digestion-resistant fraction from soybean on retarding of bile acid transport *in vitro*. *Nutrition Research & Practice* **3**(2):149–155.

Haralampu, S. (2000). Resistant starch–A review of the physical properties and biological impact of RS 3. *Carbohydr. Polym.* **41**(3):285–292.

Haralampu, S. G. (2001). In: Advanced dietary fibre technology Mccleary, pp. 413–201. Prosky, B. V., L. (Ed.). Oxford: Blackwell Science.

Hasjim, J. and Jane, J.-L. (2009). Production of resistant starch by extrusion cooking of acid-modified normal-maize starch. *J. Food Sci.* **74**(7): C556–C562.

Hizukuri, S. H., Takeda, Y., Abe, J., Hanashiro, I., Matsunobu, G. and Kiyota, H. (1997). Analytical developments: Molecular and microstructural characterization. In: Starch: Structure and Functionality. pp. 121. Frazier, P. J., Richmond, P., and Donal, A. M. (Eds.). London: Royal Society of Chemistry.

Homayouni, A., Amini, A., Keshtiban, A. K., Mortazavian, A. M., Esazadeh, K. and Pourmoradian, S. (2014). Resistant starch in food industry: A changing outlook for consumer and producer. *Starch - Starke* **6**(1–2):102–114.

Hoover, R. and Zhou, Y. (2003). In vitro and *in vivo* hydrolysis of legume starches by α-amylase and resistant starch formation in legumes–A review. *Carbohydr. Polym.* **54**(4):401–417.

Hospers, J. J., Amelsvoort, J. M. M. V. and Weststrate, J. A. (1994). Amylose-to-amylopectin ratio in pastas affects postprandial glucose and insulin responses and satiety in males. *J. Food Sci.* **59**(5):1144–1149.

Htoon, A., Shrestha, A., Flanagan, B., Lopez-Rubio, A., Bird, A., Gilbert, E. and Gidley, M. (2009). Effects of processing high amylose maize starches under controlled conditions on structural organisation and amylase digestibility. *Carbohydr. Polym.* **75**(2):236–245.

Hu, G. F. (1995). Fluorophore-assisted carbohydrate electrophoresis technology and applications. *J. Chromatogr. A* **705**(1):89–103.

Jane, J.-L. (2004). In: Chemical and Functional Properties of Food Saccharides, pp. 81–101. Tomasik, P. (Ed.). New York: CRC Press.

Jane, J.-L. (2006). Current understanding on starch granule structures. *J. Appl. Glycosci.* **53**(3):205–213.

Jane, J.-L. (2007). Structure of starch granules. *J. Appl. Glycosci.* **54**(1):31–36.

Jane, J., Chen, Y. Y., Lee, L. F., Mcpherson, A. E., Wong, K. S., Radosavljevic, M. and Kasemsuwan, T. (1999). Effects of amylopectin branch chain length and amylose content on the gelatinization and pasting properties of starch. *Cereal Chem.* **76**(5):629–637.

Jiang, H., Campbell, M., Blanco, M. and Jane, J.-L. (2010a). Characterization of maize amylose-extender (ae) mutant starches: Part II. Structures and properties of starch residues remaining after enzymatic hydrolysis at boiling-water temperature. *Carbohydr. Polym.* **80**(1):1–12.

Jiang, H., Horner, H. T., Pepper, T. M., Blanco, M., Campbell, M. and Jane, J.-L. (2010b). Formation of elongated starch granules in high-amylose maize. *Carbohydr. Polym.* **80**(2):533–538.

Jiang, H., Lio, J., Blanco, M., Campbell, M. and Jane, J.-L. (2010c). Resistant-starch formation in high-amylose maize starch during kernel development. *J. Agric. Food Chem.* **58**(13):8043–8047.

Karim, A. A., Norziah, M. and Seow, C. (2000). Methods for the study of starch retrogradation. *Food chem.* **71**(1):9–36.

Kim, N. H., Kim, J. H., Lee, S., Lee, H., Yoon, J. W., Wang, R. and Yoo, S. H. (2010). Combined effect of autoclaving-cooling and cross-linking treatments of normal corn starch on the resistant starch formation and physicochemical properties. *Starch-Stärke* **62**(7):358–363.

Lehmann, U., Jacobasch, G. and Schmiedl, D. (2002). Characterization of resistant starch type III from banana (Musa acuminata). *J. Agric. Food Chem.* **50**(18):5236–5240.

Lesmes, U., Beards, E. J., Gibson, G. R., Tuohy, K. M. and Shimoni, E. (2008). Effects of resistant starch type III polymorphs on human colon microbiota and short chain fatty acids in human gut models. *J. Agric. Food Chem.* **56**(13):5415–5421.

Leszczyñski, W. (2004). Resistant starch–Classification, structure, production. *Pol. J. Food Nutr. Sci.* **13**(54):37–50.

Lopez, H. W., Coudray, C., Bellanger, J., Levrat-Verny, M. A., Demigne, C., Rayssiguier, Y. and Remesy, C. (2000). Resistant starch improves mineral assimilation in rats adapted to a wheat bran diet. *Nutr. Res.* **20** (1):141–155.

Lopez-Rubio, A., Flanagan, B. M., Gilbert, E. P. and Gidley, M. J. (2008a). A novel approach for calculating starch crystallinity and its correlation with double helix content: A combined XRD and NMR study. *Biopolymers* **89**(9):761–768.

Lopez-Rubio, A., Flanagan, B. M., Shrestha, A. K., Gidley, M. J. and Gilbert, E. P. (2008b). Molecular rearrangement of starch during *in vitro* digestion: Toward a better understanding of enzyme resistant starch formation in processed starches. *Biomacromolecules* **9** (7):1951–1958.

Lopez-Rubio, A. and Gilbert, E. P. (2010). Neutron scattering: A natural tool for food science and technology research. *Trends Food Sci. Technol.* **20**(11–12):576–586.

Lopez-Rubio, A., Htoon, A. and Gilbert, E. P. (2007). Influence of extrusion and digestion on the nanostructure of high-amylose maize starch. *Biomacromolecules* **8**(5):1564–1572.

Luckett, C. (2012). Effect of Enzymatic Treatments on the Physiochemical Properties of Different Corn Starches. MSc. thesis, University of Arkansas.

Lunn, J. and Buttriss, J. L. (2007). Carbohydrates and dietary fibre. *Nutr. Bull.* **32**:21–64.

Lösel, D. and Claus, R. (2005). Dose-dependent effects of resistant potato starch in the diet on intestinal skatole formation and adipose tissue accumulation in the pig. *J. Vet. Med. A* **52**(5):209–212.

Mahadevamma, S., Prashanth, K. H. and Tharanathan, R. (2003). Resistant starch derived from processed legumes–Purification and structural characterization. *Carbohydr. Polym.* **54**(2):215–219.

Mangala, S. L., Malleshi, N. G. and Tharanathan, R. N. (1999b). Resistant starch from differently processed rice and ragi (finger millet). *Eur. Food Res. Technol.* **209**(1):32–37.

Mangala, S., Ramesh, H., Udayasankar, K. and Tharanathan, R. (1999a). Resistant starch derived from processed ragi (finger millet, Eleusine coracana) flour: Structural characterization. *Food chem.* **64** (4):475–479.

Mangala, S. L. and Tharanathan, R. N. (1999). Structural studies of resistant starch derived from processed (autoclaved) rice. *Eur. Food Res. Technol.* **209**(1):38–42.

Miao, M., Jiang, B. and Zhang, T. (2009). Effect of pullulanase debranching and recrystallization on structure and digestibility of waxy maize starch. *Carbohydr. Polym.* **76**(2):214–221.

Morell, M. K., Konik-Rose, C., Ahmed, R., Li, Z. and Rahman, S. (2004). Synthesis of resistant starches in plants. *J. AOAC Int.* **87**(3):740–748.

Morrison, W. R., Law, R. V. and Snape, C. E. (1993). Evidence for inclusion complexes of lipids with V-amylose in maize, rice and oat starches. *J. Cereal Sci.* **18**(2):107–109.

Mutungi, C., Onyango, C., Doert, T., Paasch, S., Thiele, S., Machill, S., Jaros, D. and Rohm, H. (2011). Long- and short-range structural changes of recrystallised cassava starch subjected to *in vitro* digestion. *Food Hydrocolloids* **25**(3):477–485.

Niba, L. L. (2002). Resistant starch: A potential functional food ingredient. *Nutr. Food Sci.* **32**(2):62–67.

Nugent, A. P. (2005). Health properties of resistant starch. *Nutr. Bull.* **30** (1):27–54.

Nunes, F. M., Lopes, E. S., Moreira, A. S. P., Simões, J., Coimbra, M. A. and Domingues, R. M. (2016). Formation of type 4 resistant starch and maltodextrins from amylose and amylopectin upon dry heating: A model study. *Carbohydr. Polym.* **141**:253–262.

Ogawa, K., Yamazaki, I., Yoshimura, T., Ono, S., Rengakuji, S., Nakamura, Y. and Shimasaki, C. (1998). Studies on the retrogradation and structural properties of waxy corn starch. *Bull. Chem. Soc. Jpn.* **71**(5):1095–1100.

Onyango, C., Bley, T., Jacob, A., Henle, T. and Rohm, H. (2006). Influence of incubation temperature and time on resistant starch type III formation from autoclaved and acid-hydrolysed cassava starch. *Carbohydr. Polym.* **66**(4):494–499.

Paramahans, S. V. and Tharanathan, R. N. (1982). Scanning electron microscopy of enzyme digested varagu starch granules. *Starch - Stärke* **34**(3):73–76.

Perera, A., Meda, V. and Tyler, R. (2010). Resistant starch: A review of analytical protocols for determining resistant starch and of factors affecting the resistant starch content of foods. *Food Res. Int.* **43** (8):1959–1974.

Pikus, S. (2005). Small-angle X-ray scattering (SAXS) studies of the structure of starch and starch products. *Fibres Text. East. Eur.* **13**(5):82–86.

Pohu, A., Putaux, J. L., Planchot, V., Buleon, A. and Colonna, P. (2004). Origin of the limited alpha-amylolysis of debranched maltodextrins crystallized in the A form: A TEM study on model substrates. *Biomacromolecules* **5**(1):119–125.

Polesi, L. F. and Sarmento, S. B. S. (2011). Structural and physicochemical characterization of RS prepared using hydrolysis and heat treatments of chickpea starch. *Starch-Stärke* **63**(4):226–235.

Raben, A., Andersen, K., Karberg, M. A., Holst, J. J. and Astrup, A. (1997). Acetylation of or beta-cyclodextrin addition to potato beneficial effect on glucose metabolism and appetite sensations. *Am. J. Clin. Nutr.* **66**(2):304–314.

Raigond, P., Ezekiel, R. and Raigond, B. (2015). Resistant starch in food: A review. *J. Sci. Food Agric.* **95**(10):1968–1978.

Reddy, C. K., Suriya, M. and Haripriya, S. (2013). Physico-chemical and functional properties of resistant starch prepared from red kidney beans (*Phaseolus vulgaris. L*) starch by enzymatic method. *Carbohydr. Polym.* **95**(1):220–226.

Robertson, J. A., Monredon, F. D. D., Dysseler, P., Guillon, F., Amado, R. and Thibault, J. F. (2000). Hydration properties of dietary fibre and resistant starch: A European collaborative study. *Lebensmittel-Wissenschaft und-Technologie* **33**(2):72–79.

Ruiz-Matute, A. I., Hernández-Hernández, O., Rodríguez-Sánchez, S., Sanz, M. L. and Martínez-Castro, I. (2010). Derivatization of carbohydrates for GC and GC-MS analyses. *J. Chromatogr. B: Anal. Technol. Biomed. Life Sci.* **879**(17–18):1226–1240.

Russell, P. L., Berry, C. S. and Greenwell, P. (1989). Characterisation of resistant starch from wheat and maize. *J. Cereal Sci.* **9**(1):1–15.

Sajilata, M. G., Singhal, R. S. and Kulkarni, P. R. (2006). Resistant starch–A review. *Compr. Rev. Food Sci. Food Saf.* **5**(1):1–17.

Samuels, R. J. (1970). X-ray diffraction methods in polymer science. In: Materials Science & Engineering, pp. 66, Alexander, L. E. (Ed.). New York: Wiley-Interscience.

Sang, Y. and Seib, P. A. (2006). Resistant starches from amylose mutants of corn by simultaneous heat-moisture treatment and phosphorylation. *Carbohydr. Polym.* **63**(2):167–175.

Schmidt, P. W. (1991). Small-sngle scattering studies of disordered, porous and fractal systems. *J. Appl. Crystallogr.* **24**(5):414–435.

Schmidt-Rohr, K. (2007). Simulation of small-angle scattering curves by numerical Fourier transformation. *J. Appl. Crystallogr.* **40**(1):16–25.

Schmiedl, D., Bauerlein, M., Bengs, H. and Jacobasch, G. (2000). Production of heat-stable, butyrogenic resistant starch. *Carbohydr. Polym.* **43** (2):183–193.

Schulz, A. G., Van Amelsvoort, J. M. and Beynen, A. C. (1993). Dietary native resistant starch but not retrograded resistant starch raises magnesium and calcium absorption in rats. *J. Nutr.* **123**(10):1724–1731.

Shamai, K., Shimoni, E. and Bianco-Peled, H. (2004). Small angle X-ray scattering of resistant starch type III. *Biomacromolecules* **5**(1):219–223.

Sharma, A., Yadav, B. S. and Ritika (2008). Resistant starch: Physiological roles and food applications. *Food Rev. Int.* **24**(2):193–234.

Shi, M. M. and Gao, Q. Y. (2011). Physicochemical properties, structure and *in vitro* digestion of resistant starch from waxy rice starch. *Carbohydr. Polym.* **84**(3):1151–1157.

Shrestha, A. K., Blazek, J., Flanagan, B. M., Dhital, S., Larroque, O., Morell, M. K., Gilbert, E. P. and Gidley, M. J. (2015). Molecular, mesoscopic and microscopic structure evolution during amylase digestion of extruded maize and high amylose maize starches. *Carbohydr. Polym.* **118**(118C):224–234.

Shukla, T. (1996). Enzyme-resistant starch: A new specialty food ingredient. *Cereal Foods World*, **40**(11):882–883.

Sievert, D., Czuchajowska, Z. and Pomeranz, Y. (1991). Enzyme-resistant starch. III. X-ray diffraction of autoclaved amylomaize VII starch and enzyme-resistant starch residues. *Cereal Chem.* **68**:86–91.

Sievert, D. and Pomeranz, Y. (1989). Enzyme-resistant starch. I. Characterization and evaluation by enzymatic, thermoanalytical, and microscopic methods. *Cereal Chem.* **66**(4):342–347.

Sievert, D. and Wursch, P. (1993). Thermal behavior of potato amylose and enzyme-resistant starch from maize. *J. Appl. Phys.* **75**(3):66–72.

Siljeström, M., Eliasson, A. C. and Björck, I. (1989). Characterization of resistant starch from autoclaved wheat starch. *Starch - Stärke* **41**(4):147–151.

Simsek, S. and El, S. N. (2012). Production of resistant starch from taro (*Colocasia esculenta* L. Schott) corm and determination of its effects on health by *in vitro* methods. *Carbohydr. Polym.* **90**(3):1204–1209.

Soest, J. J. G. V., Tournois, H., Wit, D. D. and Vliegenthart, J. F. G. (1995). Short-range structure in (partially) crystalline potato starch determined with attenuated total reflectance Fourier-transform IR spectroscopy. *Carbohydr. Res.* **279**(95):201–214.

Song, Y. and Jane, J. (2000). Characterization of barley starches of waxy, normal, and high amylose varieties. *Carbohydr. Polym.* **41**(4):365–377.

Starr, C. M., Masada, R. I., Hague, C., Skop, E. and Klock, J. C. (1996). Fluorophore-assisted carbohydrate electrophoresis in the separation, analysis, and sequencing of carbohydrates. *J. Chromatogr. A* **720**(1–2):295–321.

Suzuki, T., Chiba, A. and Yarno, T. (1997). Interpretation of small angle x-ray scattering from starch on the basis of fractals. *Carbohydr. Polym.* **34**(4):357–363.

Tharanathan, M. and Tharanathan, R. (2001). Resistant starch in wheat-based products: Isolation and characterisation. *J. Cereal Sci.* **34**(1):73–84.

Thérien, H. (2007). Study of hydration of cross-linked high amylose starch by solid state 13C NMR spectroscopy. *Carbohydr. Res.* **342**(11):1525–1529.

Thompson, D. B. (2000). Strategies for the manufacture of resistant starch. *Trends Food Sci. Technol.* **11**(7):245–253.

van Soest, J. J. G., De Wit, D., Tournois, H. and Vliegenthart, J. F. G. (1994). Retrogradation of potato starch as studied by Fourier transform infrared spectroscopy. *Starch - Stärke* **46**(12):453–457.

van Soest, J. J., Tournois, H., de Wit, D. and Vliegenthart, J. F. (1995). Short-range structure in (partially) crystalline potato starch determined with attenuated total reflectance Fourier-transform IR spectroscopy. *Carbohydr. Res.* **279**:201–214.

Wang, Z. G., Hsiao, B. S. and Murthy, N. S. (2007). Comparison of intensity profile analysis and correlation function methods for studying the lamellar structures of semi-crystalline polymers using small-angle X-ray scattering. *J. Appl. Crystallogr.* **33**(3):690–694.

Wang, Y. J., Kozlowski, R. and Delgado, G. A. (2001). Enzyme resistant dextrins from high amylose corn mutant starches. *Starch-Stärke* **53**(1):21–26.

Wang, J., Tang, X. J., Chen, P. S. and Huang, H. H. (2014). Changes in resistant starch from two banana cultivars during postharvest storage. *Food chem.* **156**:319–325.

Weickert, M., Mohlig, M., Koebnick, C., Holst, J., Namsolleck, P., Ristow, M., Osterhoff, M., Rochlitz, H., Rudovich, N. and Spranger, J. (2005). Impact of cereal fibre on glucose-regulating factors. *Diabetologia* **48**(11):2343–2353.

Williamson, G., Belshaw, N. J., Self, D. J., Noel, T. R., Ring, S. G., Cairns, P., Morris, V. J., Clark, S. A. and Parker, M. L. (1992). Hydrolysis of A-and B-type crystalline polymorphs of starch by α-amylase, β-amylase and glucoamylase 1. *Carbohydr. Polym.* **18**(3):179–187.

Won, C. Y., Chu, C. C. and Yu, T. J. (1997). Synthesis of starch-based drug carrier for the control/release of estrone hormone. *Carbohydr. Polym.* **32**(3):239–244.

Wu, A. C., Li, E. P. and Gilbert, R. G. (2014). Exploring extraction/dissolution procedures for analysis of starch chain-length distributions. *Carbohydr. Polym.* **114**(1):36–42.

Xie, X. and Liu, Q. (2004). Development and physicochemical characterization of new resistant citrate starch from different corn starches. *Starch - Stärke* **56**(8):364–370.

Xie, X., Liu, Q. and Cui, S. W. (2006). Studies on the granular structure of resistant starches (type 4) from normal, high amylose and waxy corn starch citrates. *Food Res. Int.* **39**(3):332–341.

Yang, Z., Gu, Q., Lam, E., Tian, F., Chaieb, S. and Hemar, Y. (2016). In situ study starch gelatinization under ultra-high hydrostatic pressure using synchrotron SAXS. *Food Hydrocolloids* **56**:58–61.

Yao, N., Paez, A. V. and White, P. J. (2009). Structure and function of starch and resistant starch from corn with different doses of mutant amylose-extender and floury-1 alleles. *J. Agric. Food Chem.* **57**(5):2040–2048.

Yin, H. L., Karim, A. A. and Norziah, M. H. (2007). Effect of pullulanase debranching of sago (Metroxylon sagu) starch at subgelatinization temperature on the yield of resistant starch. *Starch - Stärke* **59**(1):21–32.

Yonekura, L. and Suzuki, H. (2005). Effects of dietary zinc levels, phytic acid and resistant starch on zinc bioavailability in rats. *Eur. J. Nutr.* **44**(6):384–391.

Yuryev, V. P., Krivandin, A. V., Kiseleva, V. I., Wasserman, L. A., Genkina, N. K., Fornal, J., Blaszczak, W. and Schiraldi, A. (2004). Structural parameters of amylopectin clusters and semi-crystalline growth rings in wheat starches with different amylose content. *Carbohydr. Res.* **339**(16):2683–2691.

Zabar, S., Shimoni, E. and Bianco-Peled, H. (2008). Development of nanostructure in resistant starch type III during thermal treatments and cycling. *Macromol. Biosci.* **8**(2):163–170.

Zeng, S., Wu, X., Shan, L., Zeng, H., Xu, L., Yi, Z. and Zheng, B. (2015). Structural characteristics and physicochemical properties of lotus seed resistant starch prepared by different methods. *Food Chem.* **186**:213–222.

Zhang, J., Chen, F., Liu, F. and Wang, Z. W. (2010). Study on structural changes of microwave heat-moisture treated resistant Canna edulis Ker starch during digestion *in vitro*. *Food Hydrocolloids* **24**(1):27–34.

Zhang, B., Chen, L., Xie, F., Li, X., Truss, R. W., Halley, P. J., Shamshina, J. L., Rogers, R. D. and Mcnally, T. (2015). Understanding the structural disorganization of starch in water-ionic liquid solutions. *Phys. Chem. Chem. Phys.* **17**(21):13860–13871.

Zhang, Y., Zeng, H., Wang, Y., Zeng, S. and Zheng, B. (2014). Structural characteristics and crystalline properties of lotus seed resistant starch and its prebiotic effects. *Food chem.* **155**:311–318.

Zhao, X. H. and Yang, L. (2009). Resistant starch prepared from high-amylose maize starch with citric acid hydrolysis and its simulated fermentation *in vitro*. *Eur. Food Res. Technol.* **228**(6):1015–1021.

Zhou, Z., Cao, X. and Zhou, J. Y. (2013). Effect of resistant starch structure on short-chain fatty acids production by human gut microbiota fermentation *in vitro*. *Starch - Stärke* **65**(5–6):509–516.

Zhou, Y., Meng, S., Chen, D., Zhu, X. and Yuan, H. (2014). Structure characterization and hypoglycemic effects of dual modified resistant starch from indica rice starch. *Carbohydr. Polym.* **103**:81–86.

Zobel, H. (1988). Starch crystal transformations and their industrial importance. *Starch-Stärke* **40**(1):1–7.